Isolation and culture of primary trophoblast cells. Trophoblast cells were isolated from the placentas of early human pregnancies as reported previously [11]. We repeated experiments in this investigation through the use of more than 20 placentas from volunteers at 7 to 9 gestational weeks. Briefly, minced villous tissues were digested with 0.125% trypsin (Invitrogen Corporations, Carlsbad, CA), 0.42 mM of $MgSO_4$, and 20 U/ml of DNase type 1 (Invitrogen Corporations) and passed through mesh (100 μm pore size, Invitrogen Corporations). The collected cells separated over 40%/25%/0% Percoll density gradients (Sigma–Aldrich Inc., St. Louis, MO; 4 ml per layer in a 15-ml conical tube). After centrifugation at 800g for 20 min, cells positioned at the interface between the 25 and 40% Percoll layers were collected. The isolated cells were seeded in a plate precoated with type 4 collagen (Becton–Dickinson, Franklin Lakes, NJ, USA) in 5% CO_2/20% O_2 at 37 °C in defined keratinocyte serum free medium (dKSFM; Invitrogen Corporations). In this study, the additional magnetic bead purification described previously [11] was not performed, allowing increased cellular yields. Instead, purity of the isolated primary trophoblast cells was addressed by immunocytochemistry using anti-cytokeratin type 7 LP5K (1 μg/ml, Immunologicals direct, Oxfordshire, UK) and anti-vimentin V9 (5 μg/ml, DAKO, Kyoto, Japan) mAbs.

Immunohistochemistry. Early gestational placentas were obtained from elective terminations of pregnancy performed at 7–9 weeks of gestation. Tissue segments were snap-frozen in liquid nitrogen and cryosectioned at 7 μm intervals (Leica, Nußloch, Germany). Slides were fixed in methanol–acetone and incubated in 0.03% H_2O_2 (DAKO, Kyoto, Japan) for 10 min. After blocking, slides were incubated with primary antibodies [anti-CD1d NOR3.2 (Abcam Inc., Cambridge, MA), anti-CD9 P1/33/2 (DAKO, Kyoto, Japan) or anti-HLA-G 87G (kind gift, Daniel E. Geraghty, Fred Hutchinson Cancer Research Center, Seattle, WA)] for 30 min at room temperature. Isotype- and concentration-matched mouse IgGs (IgG1 for NOR3.2 and P1/33/2, IgG2 for 87G, DAKO, Kyoto, Japan) served as negative controls. After washing, slides were incubated with a peroxidase-conjugated polymer-labeled goat anti-mouse immunoglobulin antibody for 30 min at room temperature (polymer-immunocomplex method; DAKO). The reaction was visualized using a diaminobenzidine solution containing H_2O_2 in TBS (DAKO).

Flow cytometry. Single-color flow cytometry was performed to determine cell-surface CD1d expression patterns. Trophoblast cells were detached from culture plates with 0.05% EDTA in TBS and incubated with anti-CD1d NOR3.2 or anti-HLA-G 87G mAbs (1 μg/ml) in PBS for 30 min. For indirect staining experiments, cells were incubated with RPE anti mouse IgG (Dako Cytomation, Glostrup, Denmark) for 30 min. Controls were exposed to an isotype-matched irrelevant mAb (Dako Cytomation, 1 μg/ml). Double-color flow cytometry was also performed to address co-expression of CD1d and CD9 or HLA-G. Detached trophoblast cells were incubated with NOR3.2 or isotype-matched control IgG (1 μg/ml) for 30 min. After washing, the cells were incubated with Cy5-conjugated anti-mouse IgG. Cells were again washed in PBS and incubated with FITC-conjugated mAbs (CD9-FITC for CD9, MEMG1-FITC for HLA-G, or IgG-FITC for control) (1 μg/ml) for 30 min. After washing, the cells were subjected to flow cytometry analysis for PC5 and FITC.

Quantitative RT-PCR. Quantitative RT-PCR was performed for CD1d in cultured trophoblast cells. Total RNA was isolated from the primary cultured trophoblast cells using the RNeasy kit (Qiagen Inc., Valencia, CA). Two micrograms of total RNA were subjected to reverse transcription using the ReverTraAce kit (TOYOBO, Tsuruga, Japan) according to the manufacturer's instructions. About 0.2–2 μl of each RT-reaction was used for quantitative PCR using the Light Cycler system (Roche Diagnostics, Lewes, UK) and the following primer pairs: CD1d-forward 5′-AAGAAGCAAG TGAAGCCCAA-3′, -reverse 5′-CCACTTCACCCATACAGGCT-3′; and β-actin-forward 5′-CGACAACGGCTCCGGCATGTGC-3′, -reverse 5′-CGTCACCGGAGTCCATCACGATG C-3′. These primer pairs were designed using "primer3" primer-making software (http://workbench.sdsc.edu/). β-Actin mRNA levels were quantified in each sample as an internal control to allow normalization. To allow highly quantitative analysis, RT-quantitative PCR was repeated at least five times.

Cytokine exposure and monoclonal antibody neutralization of TGF-β1. At 48 h after seeding, cultured trophoblasts were exposed to human recombinant TGF-β1 or IFN-γ (R&D Systems, Minneapolis, MN; 0.3 and 1.0 ng/ml, respectively) for an additional 48 h to use RT-PCR or flow cytometry. Culture media was changed daily and cytokines newly added with media changes. For TGF-β1 neutralization, an anti-TGF-β1 mAb (R&D Systems; 5 μg/ml working concentration) was added to the medium at 48 h after seeding. After 48 h of incubation in the presence of the anti-TGF-β1 mAb, the total RNA in cultured trophoblasts was collected for RT-PCR analysis.

ELISA for TGF-β1. Culture medium of primary EVT cells was collected at 48, 72, and 96 h of culture. Levels of secreted TGF-β1 were quantified using solid phase sandwich ELISAs (R&D Systems) according to the manufacturer's instructions. A standard curve was produced using absorbance measurements at 450 nm for standard samples. Each unknown sample was similarly measured and plotted on the standard curve.

Statistical analysis. Quantitative PCR data are presented as means ± standard deviations. These experiments were performed independently three times, and each experiment was repeated in four different patients. mRNA levels were compared between those at each dose or time by ANOVA. A p-value of <0.05 was considered significant.

Results

Expression and distribution of CD1d in human placenta from normal early pregnancies

To assess the localization of CD1d in human placenta, sections of snap-frozen placental tissues from early pregnancies (7–9 gestational weeks) were immunostained using an anti-CD1d mAb (NOR3.2). Since CD1d had been previously documented in EVT cells [4], sections of tissues from the maternal-fetal interface that contained anchoring villi were used. EVT derived from anchoring villi typically form aggregates, called cell columns, as they invade into the decidua (Fig. 1). They then stream into the decidua, where they are called interstitial trophoblast cells, and into the maternal decidual vessels (endovascular trophoblast cells). Classical EVT are positive for CD9 and HLA-G, so immunostaining for these products was performed on serial sections to confirm the presence of EVT cells. CD1d was detected in the trophoblast cells of early gestation placental specimens (Fig. 1A and A′). Strong immunoreactivity for CD1d was observed in those villous cytotrophoblast cells located along the inner layer of the epithelium of anchoring villi. Those EVT cells forming the proximal trophoblast cell columns (proximal EVT cells) demonstrated the strongest immunoreactivity for CD1d noted in the placenta. EVT cells forming distal trophoblast cell columns (distal EVT cells) that invade into the decidua and differentiate into interstitial or endovascular trophoblast cells strongly expressed both CD9 and HLA-G, as expected. Interestingly, the CD1d immunoreactivity of the EVT cells decreased as level of invasion/differentiation increased and was barely detectable in the most distal EVT cells. Immunostaining patterns for CD9 and HLA-G were inverse to those for CD1d, positively correlating with the level of invasion/differentiation (Fig. 1B for CD9 and Fig. 1C for HLA-G). CD1d immunoreactivity was not observed in syncytiotrophoblast, decidual or stromal cells.

Decreased cell-surface expression of CD1d in EVT cells occurs in the absence of decidual interactions

We then confirmed cell surface expression of CD1d in vitro in primary cultured trophoblast cells using flow cytometry. Culture purity was assessed using anti-cytokeratin type 7 and anti-vimentin immunocytochemistry. The percentage of contaminating stromal cells (cytokeratin type 7 negative and vimentin positive) was less than 5% at 96 h of culture (Fig. 2A). In this *in vitro* system, we had previously shown that cultured trophoblast cells retained characteristics of proximal EVT cells until at least 48 h of culture (expressing CD9 and HLA-G) [11]. Here, isolated trophoblast cells were similarly cultured for 48 h but co-stained with an anti-CD1d (NOR3.2) mAb and either an anti-HLA-G (87G) or an anti-CD9 mAb (Fig. 2B). Double staining and FACS analysis demonstrated that the majority of cells expressed CD1d and HLA-G (Fig. 2B, left) or CD1d and CD9 (Fig. 2B, center). Since both HLA-G and CD9 are well-described cell-surface markers for EVT cells, the isolated trophoblast cells had differentiated into EVT cells by 48 h of culture. These data support immunohistochemical data showing that CD1d was present on the cell surface of the proximal EVT cells which were immunoreactive for both HLA-G and CD9.

To quantitatively assess whether trophoblast differentiation was associated with a decrease in cell surface CD1d expression, cultured EVT cells were harvested at several time points post-isolation and analyzed by flow cytometry. We have previously demonstrated that our primary culture system allows *in vitro* trophoblast differentiation [11]. Cytotrophoblast cells exhibit phenotypic alterations that characterize first cells of the proximal EVT

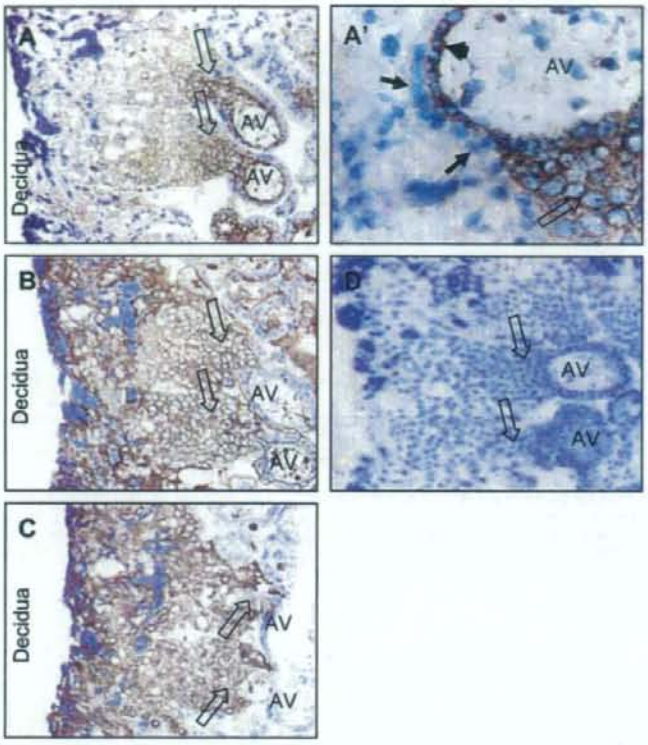

Fig. 1. CD1d is expressed on human cytotrophoblast cells and decreases with EVT invasion. Snap-frozen and fixed placental tissue from a 9 wk human placenta was serially sectioned across the maternal-fetal interface and stained for CD1d (A); CD9 (a marker for EVT cells) (B); HLA-G (a marker for EVT differentiation) (C) and an isotype-control for anti-CD1d mAb (D) (100×). As positioned, invasion is initiated at the anchoring villi (AV) and proceeds to the left, towards the decidua. (A') A magnification of the section serial to that shown in (A) (400×). Open arrows indicate trophoblast cell columns. Closed arrowheads indicate villous cytotrophoblast. Small arrows indicate syncytiotrophoblast. These data were reproduced in samples from four different patients.

cell column, then those of the distal EVT cell column and finally those of the interstitial EVT [11]. Consistent with our immunohistochemical data (Fig. 1B and C), those interstitial EVT cells that diffusely invade the maternal decidua *in vivo* are known to express specific cell surface markers, including integrin-α1, HLA-G, and CD9 [12]. Fig. 2 reconfirms that cytotrophoblast cells differentiated into proximal EVT cells by 48 h of culture using our primary trophoblast culture model. Flow cytometry revealed that proximal cell column EVT cells at 48 h of culture strongly expressed CD1d at the cell surface (Fig. 3A, left top panel). The number of CD1d-bearing EVT cells decreased dramatically by 96 h of culture (Fig. 3A, left panels). In turn, HLA-G-bearing EVT cells increased with time in culture, indicating the proximal EVT cells differentiated into invading EVT cells during 48–96 h of culture (Fig. 3A, right panels). Cell-surface CD1d in EVT cells decreased as the cells differentiated during *in vitro* culture. This decrease recapitulates that seen occurring with invasion *in vivo*, but occurs in the absence of interactions with maternal decidua.

TGF-β1 downregulates the transcription of CD1d in cultured human EVT

To address mechanisms by which cell-surface CD1d is downregulated in EVT cells, we employed quantitative RT-PCR to investigate alterations in CD1d mRNA levels in cultured EVT cells over time. When compared to the 48 h control time point, CD1d mRNA levels decreased at 72 h and 96 h of culture (Fig. 3B). CD1d transcriptional changes paralleled cell-surface expression patterns seen with flow cytometry, indicating that downregulation of CD1d occurs at least at the level of transcription.

Since CD1d downregulation in EVT cells coincides with EVT differentiation *in vitro*, we investigated the possibility of autocrine modulation through cytokines. We here focused on the immunosuppressive cytokine, TGF-β1, which is reported to be secreted from EVT cells [13]. We addressed secretion of TGF-β1 by EVT using ELISA (Fig. 3C). TGF-β1 levels in EVT culture media increased over time, indicating that TGF-β1 is secreted from cultured EVT cells and accumulates as the cells differentiate. To examine the direct effect of TGF-β1 on CD1d expression, EVT cells at 48 h of culture were exposed to TGF-β1 or to IFN-γ (Fig. 4A and B). IFN-γ induced CD1d transcription as expected [14], but TGF-β1 suppressed CD1d transcription in a dose-dependent fashion (Fig. 4A). These alterations in CD1d expression were also shown at protein level by flow cytometry (Fig. 4B).

To confirm the specificity of the TGF-β1 effect, an anti-TGF-β1 neutralizing mAb or an isotype-matched mAb control was added in neutralization assays. EVT cells at 48 h after isolation were cultured for an additional 48 h in the presence of TGF-β1 neutralizing or control antibodies with no media changes. Messenger RNA was collected after 48 h. Quantitative RT-PCR demonstrated that the transcription of CD1d was recovered upon TGF-β1 neutralization (Fig. 4B).

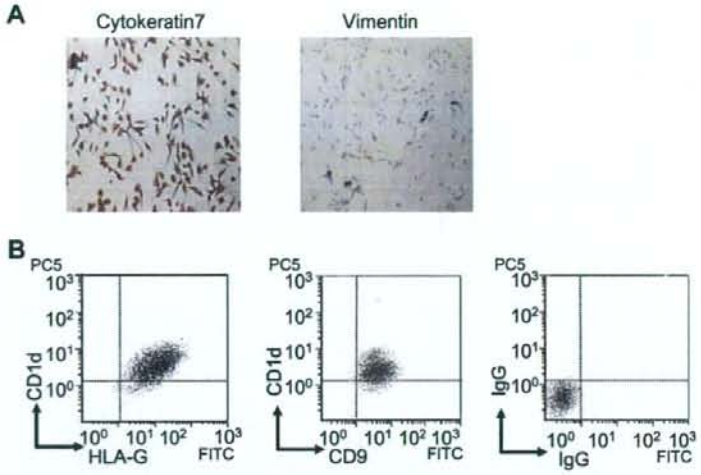

Fig. 2. CD1d and HLA-G are expressed on the surface of EVT in culture. (A) Purity of cultured EVT cells was assessed by immunocytochemistry using anti-cytokeratin type7 (left) and anti-vimentin (right) antibodies. The percentage of contaminating stromal cells (cytokeratin type 7 negative and vimentin positive) was less than 5% at 96 h of culture. (100×). (B) Cell surface expression was assessed by flow cytometry of the trophoblast cells cultured *in vitro* for 48 h and double-stained for (left) HLA-G (a marker for EVT differentiation) and CD1d or (center) CD9 (a marker for EVT cells) and CD1d. Isotype-matched controls are represented in the plot on the right. These data were reproduced in samples from at least four different patients.

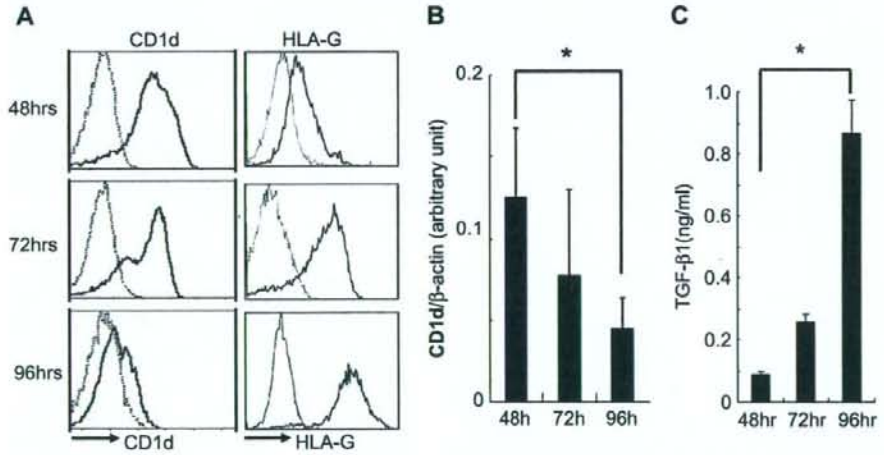

Fig. 3. Time-dependent alterations in cell-surface expression of CD1d and HLA-G and in CD1d transcription in cultured EVT cells. (A) Trophoblast cells were cultured for 48, 72, and 96 h, immunostained with anti-CD1d NOR3.2 (left) and anti-HLA-G 87G (right) antibodies and analyzed by flow cytometry. Isotype-matched antibody controls are depicted as dotted lines in each histogram. These data were reproduced in samples from at least five different patients. (B) Cultured trophoblast cells were harvested at 48, 72, and 96 h. Isolated mRNA was subjected to quantitative RT-PCR using primers specific for CD1d. Samples were normalized to β-actin ($n = 4$). (C) EVT cells were cultured with daily media changes until 48 h after seeding then cultured for additional 48 h without media changes. Culture media was collected at 48, 72, and 96 h of culture. Levels of secreted TGF-β1 were measured by sandwich ELISA ($n = 6$). Asterisks indicate statistical significance ($p < 0.05$) when analyzed by ANOVA.

Discussion

Here, we present several major findings concerning CD1d at the human maternal-fetal interface. First, we demonstrate that CD1d expression is regulated *in vivo* in a trophoblast differentiation-dependent manner. Morphologic examination of early gestational tissues from the maternal-fetal interface reveals characteristics of normal trophoblast invasion from anchoring villi into the maternal decidua. Immunohistochemical data reveal a clear inverse association between CD1d expression and invasion into the maternal decidua. CD1d was not expressed in syncytiotrophoblast cells that serve as the initial points of contact between fetal and maternal tissues. iNKT cells at this site are of maternal origin and are present only in the maternal decidua and in the maternal blood bathing areas of placental villi that are completely enveloped in syncytiotrophoblast cells [1]. The lack of CD1d expression in syncytiotrophoblast, even those in anchoring villi, may protect the early placenta from interactions with iNKT cells. This could serve to in-

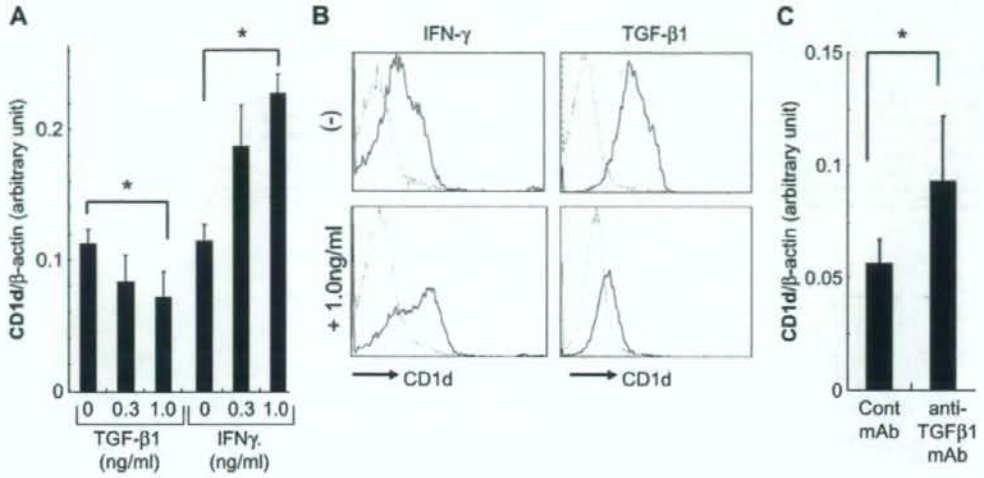

Fig. 4. Alterations in CD1d expression after exposure of cultured EVT to cytokines. (A and B) EVT cells were cultured for 48 h after seeding then exposed to TGF-β1 or IFN-γ for additional 48 h with media changes. Cells were harvested for quantitative RT-PCR using primers specific for CD1d (A) and for flow cytometry using anti-CD1d NOR3.2 mAb (B). Samples were normalized to β-actin for (A) ($n = 4$). (C) EVT cells were cultured for 48 h then exposed to a TGF β1-neutralizing mAb to for 48 h without media changes. Control cells were exposed to an isotype-matched control mAb. Cells were harvested for quantitative RT-PCR using primers specific for CD1d. Samples were normalized to β-actin ($n = 4$).

hibit the massive pro-inflammatory reaction that might result if all CD1d-bearing villous cytotrophoblast cells were exposed to decidual iNKT cells. Instead, the EVT expressed CD1d, with immunoreactivity strongest in cells located proximally in the trophoblast cell columns. Here CD1d and iNKT cells may make initial interactions during placental formation, a site where a localized pro-inflammatory reaction seems necessary for appropriate invasion of EVT into the decidua [2]. Boyson et al. have reported the importance of decidual iNKT cells and pro-inflammatory cytokines in human pregnancy [4]. CD1d-mediated activation of iNKT cells may play a critical role in creating this inflammatory microenvironment through rapid downstream cytokine production and release. Still, since massive activation of iNKT cells induces pregnancy loss [9,10] the activation of decidual iNKT cells must be tightly regulated.

Other studies have demonstrated the presence of CD1d at the human maternal-fetal interface [4,15]. However, the lack of facile *in vitro* trophoblast culture systems has limited spatiotemporal studies on placental CD1d localization and function. Our in vivo data indicated that CD1d expression in EVT decreases at distal locations within the trophoblast cell columns, sites where interstitial EVT cells are closely opposed to a great number of decidual stromal cells and infiltrating decidual immune cells (including decidual iNKT cells). This pattern differs from that for HLA-G, a cell-surface molecule whose expression increases with increasing levels of EVT invasion. Our supporting findings in an *in vitro* trophoblast cell culture model mimic the differentiation of EVT that occurs with decidual invasion *in vivo* [11]. Using this system, flow cytometry confirmed a decrease in cell surface expression of CD1d with EVT differentiation/invasion. Quantitative RT-PCR then revealed that CD1d downregulation occurred at least at the level of transcription. These highly purified EVT cultures also allow us to surmise that direct EVT/decidual interactions are not necessary for the decreases in CD1d that occur with EVT differentiation.

Several reports have shown that placental TGF-β1 is derived from decidual $CD56^{bright}CD16^{-}$NK cells [12] and EVT cells [13] and that extracellular TGF-β1 accumulates near the distal trophoblast cell columns [16]. In our study, cultured EVT cells secrete TGF-β1 in the absence of interactions with maternal decidua. *In vivo* TGF-β1 may accumulate at the maternal-fetal interface, due to a combination of autocrine and paracrine secretion from differentiated EVT cells and activated decidual NK cells. We hypothesize that TGF-β1-mediated downregulation of CD1d may be involved in this mechanism. Exposure of differentiating EVT in culture to exogenous TGF-β1, combined with TGF-β1 antibody neutralization assays, allowed demonstration that TGF-β1 specifically downregulated CD1d expression by EVT at the transcriptional level. In contrast, exposure of cultured EVT to IFN-γ resulted in a concentration-dependent increase in CD1d expression. Taken entirety, the CD1d expression in EVT cells may be regulated by the relative proportions of these functionally opposing cytokines and this may play a role in regulation of decidual iNKT cells in maternal-fetal interface.

References

[1] A.L. Mellor, D.H. Munn, Immunology at the maternal-fetal interface: lessons for T cell tolerance and suppression, Annu. Rev. Immunol. 18 (2000) 367–391.
[2] E.R. Norwitz, D.J. Schust, S.J. Fisher, Implantation and the survival of early pregnancy, N. Engl. J. Med. 345 (2001) 1400–1408.
[3] J.S. Hunt, M.G. Petroff, R.H. McIntire, C. Ober, HLA-G and immune tolerance in pregnancy, FASEB J. 19 (2005) 681–693.
[4] J.E. Boyson, B. Rybalov, L.A. Koopman, M.A. Exley, S.P. Balk, F.K. Racke, F. Schatz, R. Masch, S.B. Wilson, J.L. Strominger, CD1d and invariant NKT cells at the human maternal-fetal interface, Proc. Natl. Acad. Sci. USA 99 (2002) 13741–13746.
[5] M. Taniguchi, T. Nakayama, Recognition and function of Valpha14 NKT cells, Semin. Immunol. 12 (2000) 543–550.
[6] J.E. Gumperz, C. Roy, A. Makowska, D. Lum, M. Sugita, T. Podrebarac, Y. Koezuka, S.A. Porcelli, S. Cardell, M.B. Brenner, S.M. Behar, Murine CD1d-restricted T cell recognition of cellular lipids, Immunity 12 (2000) 211–221.
[7] K. Sonoda, M. Taniguchi, J. Stein-Streilein, Long-term survival of corneal allografts is dependent on intact CD1d-reactive NKT cells, J. Immunol. 168 (2002) 2028–2034.
[8] K. Seino, K. Fukao, K. Muramoto, K. Yanagisawa, Y. Takada, S. Kakuta, Y. Iwakura, L. Van Kaer, K. Takeda, T. Nakayama, M. Taniguchi, H. Bashuda, H. Yagita, K. Okumura, Requirement for natural killer T (NKT) cells in the induction of allograft tolerance, Proc. Natl. Acad. Sci. USA 98 (2001) 2577–2581.
[9] K. Ito, M. Karasawa, T. Kawano, T. Akasaka, H. Koseki, Y. Akutsu, E. Kondo, S. Sekiya, K. Sekikawa, M. Harada, M. Yamashita, T. Nakayama, M. Taniguchi,

Involvement of decidual Valpha14 NKT cells in abortion, Proc. Natl. Acad. Sci. USA 97 (2000) 740–744.
[10] J.E. Boyson, N. Nagarkatti, L. Nizam, M.A. Exley, J.L. Strominger, Gestation stage-dependent mechanisms of invariant natural killer T cell-mediated pregnancy loss, Proc. Natl. Acad. Sci. USA 103 (2006) 4580–4585.
[11] T. Nagamatsu, T. Fujii, T. Ishikawa, T. Kanai, H. Hyodo, T. Yamashita, Y. Osuga, M. Momoeda, S. Kozuma, Y. Taketani, A primary cell culture system for human cytotrophoblasts of proximal cytotrophoblast cell columns enabling in vitro acquisition of the extra-villous phenotype, Placenta 25 (2004) 153–165.
[12] P.P. Jokhi, A. King, A.M. Sharkey, S.K. Smith, Y.W. Loke, Screening for cytokine messenger ribonucleic acids in purified human decidual lymphocyte populations by the reverse-transcriptase polymerase chain reaction, J. Immunol. 153 (1994) 4427–4435.
[13] A. King, P.P. Jokhi, S.K. Smith, A.K. Sharkey, Y.W. Loke, Screening for cytokine mRNA in human villous and extravillous trophoblasts using the reverse-transcriptase polymerase chain reaction (RT-PCR), Cytokine 7 (1995) 364–371.
[14] M. Skold, X. Xiong, P.A. Illarionov, G.S. Besra, S.M. Behar, Interplay of cytokines and microbial signals in regulation of CD1d expression and NKT cell activation, J. Immunol. 175 (2005) 3584–3593.
[15] H.J. Jenkinson, S.D. Wainwright, K.L. Simpson, A.C. Perry, P. Fotiadou, C.H. Holmes, Expression of CD1d mRNA transcriptions in human choriocarcinoma cell lines and placentally derived trophoblast cells, Immunology 96 (1996) 649–655.
[16] H. Simpson, S.C. Robson, J.N. Bulmer, A. Barber, F. Lyall, Transforming growth factor beta expression in human placenta and placental bed during early pregnancy, Placenta 23 (2002) 44–58.

Immunology and Cell Biology (2008), 1–6

www.nature.com/icb

ORIGINAL ARTICLE

Prolactin can modulate CD4+ T-cell response through receptor-mediated alterations in the expression of T-bet

Ayako Tomio[1,4], Danny J Schust[2,3,4], Kei Kawana[1,2,3], Toshiharu Yasugi[1], Yukiko Kawana[1,2], Shruthi Mahalingaiah[3], Tomoyuki Fujii[1] and Yuji Taketani[1]

Low-dose prolactin induces proinflammatory responses and antibody production, whereas high-dose prolactin suppresses these responses. Mechanisms for these opposing effects remain incompletely defined. We have previously demonstrated that T-bet, a key transcription factor directing T helper type 1 inflammatory responses, is regulated by female steroid hormones in human mucosal epithelial cells via Stat1 and 5 pathways. T-bet was also modulated in a CD4+ T cell line by prolactin exposure. Prolactin rapidly induced T-bet transcription through phosphorylation of JAK2 and Stat5, but not Stat1. Phosphorylated Stat5 then bound to the T-bet regulatory region. These effects were weaker with high-dose prolactin exposures. Upon long-term prolactin exposure, low-dose prolactin induced T-bet expression, whereas high-dose prolactin tended to suppress it. Prolactin induced the suppressors of cytokine signaling (SOCS) 1 and 3 in a dose-dependent manner. With high-dose exposure, this was associated with an inhibition of the phosphorylation of T-bet regulatory region-bound Stat5. Further, the dose-dependent prolactin effects on T-bet expression were confirmed in murine primary CD4+ T cells. These data suggest that the divergent immune effects of low- and high-dose prolactin may involve modulation of T-bet and alterations in the balance of the prolactin/JAK2/Stat5 and the prolactin/SOCS1 and 3 pathways.
Immunology and Cell Biology advance online publication, 15 April 2008; doi:10.1038/icb.2008.29

Keywords: CD4+ T cells; JAK2; prolactin; SOCS; Stat; T-bet

Prolactin (PRL) is a polypeptide hormone with multiple physiological functions, including maintenance of pregnancy, development of the mammary glands, fluid homeostasis and immune modulation.[1–3] PRL receptor (PRLR)-deficient mice develop normally functioning conventional cellular and humoral immune systems.[4] Although PRLR and PRL may not be essential for development of the immune system, they may still be important modulators of its responses. PRL has been reported to alter the cellular and humoral arms of the immune system.[1] It can stimulate and inhibit immune responses, with type of response related to prolactin dosage.[1,2] The mechanisms responsible for these opposing effects remain undefined.

PRL is a classical pituitary hormone, but it is also produced by the decidualized endometrium. Within the endometrium, prolactin acts independently of hypothalamic/pituitary feedback. Endometrial synthesis begins in the mid-secretory phase of the human menstrual cycle and continues throughout the majority of pregnancy, resulting in markedly elevated levels of PRL in the maternal serum throughout human gestation.[5,6] High-dose PRL enhances B-cell activity and suppresses natural killer cell-mediated cytotoxic activity *in vivo*.[1] This suggests that high-dose PRL may promote the development and/or function of T helper type 2 (Th2) cells and suppress Th1 and innate immune responses. To this point, high-dose PRL (100 ng ml^{-1}) inhibits the expression of interferon regulatory factor (IRF)-1, a key transcription factor driving the Th1 phenotype in T cells.[7,8] In contrast, low-dose PRL (10 ng ml^{-1}) transiently induces IRF-1 in the nonpregnant human endometrium[9] and promotes the production of Th1 cytokines (interferon (IFN)-γ and interleukin (IL)-12) by human whole blood cells.[7,10]

Differentiation of naive T helper cells along the inflammatory Th1 pathway is also directed by a transcriptional factor called T-bet.[11] T-bet induces chromatin remodeling of the IFN-γ locus in Th1 cells.[12] Tyrosine phosphorylated T-bet also binds to a transcription factor that upregulates the production of Th2 cytokines, called GATA-3. By binding GATA-3, T-bet interferes with the interactions of GATA-3 and its target DNA.[13] In short, T-bet induces IFN-γ production while inhibiting the expression of Th2 cytokines.[11,12] T-bet is expressed in lymphoid cells, in a diverse array of the antigen-presenting cells (APCs; monocytes, macrophages, dendritic cells (DCs), myeloid cells)[14,15] and in epithelial cells of the human reproductive tract.[16]

The Stat (signal transducers and activators of transcription) proteins are latent cytoplasmic transcription factors that are activated via receptors for cytokines, growth factors and hormones. Stat1 regulates

[1]Department of Obstetrics and Gynecology, Faculty of Medicine, University of Tokyo, Tokyo, Japan; [2]Department of Obstetrics and Gynecology, Division of Reproductive Biology, Boston Medical Center, Boston University School of Medicine, Boston, MA, USA and [3]Department of Obstetrics, Gynecology, and Reproductive Biology, Brigham and Women's Hospital, Harvard Medical School, Boston, MA, USA
Correspondence: Dr K Kawana, Department of Obstetrics and Gynecology, Faculty of Medicine, University of Tokyo, 7-3-1 Hongo, Bunkyo-ku, Tokyo 113-8655, Japan.
E-mail: kkawana-tky@umin.ac.jp
[4]These authors contributed equally to this work.
Received 28 December 2006; revised 12 March 2008; accepted 13 March 2008

T-bet expression in lymphoid and DCs through IFN-γ receptor/janus kinase (JAK) 2 signaling.[17] Stat4, synergistic with IL-12 receptor-β2 (IL-12Rβ2), is essential for Th1 development in naive T cells.[12] However, the IL-12Rβ/Stat4 pathway is not specifically essential for IFN-γ-induced T-bet expression in either T cells or APCs. We have previously demonstrated that Stat5 is involved in the regulation of T-bet expression in endometrial epithelial cells (EECs).[16] In EECs, Stat1 and 5, but not Stat3 and 4, bind to the T-bet regulatory region (TRR) at the site of an IFN-γ-activated sequence (GAS) element and thereby activate T-bet transcription. Further, the Stat1 and 5 pathways are modified by exposure to the Th1 cytokines, IFN-γ and IL-15, and by exposure to the steroid hormones, estrogen and progesterone. Signaling through the cytokine receptors utilizes JAK2 for phosphorylation of Stat1 and 5 prior to their binding to the TRR; signaling through the steroid hormone receptors does not.[16]

Prolactin receptor is a member of the cytokine receptor superfamily. It is expressed on the cell surfaces of a diverse array of cells involved in immune responses, including both lymphoid and nonlymphoid derivatives. Among hematopoietic cells, PRLR has its greatest expression level on B cells, followed closely by macrophage, and finally by T cells.[18] Like signaling pathways used by more classical members of the cytokine receptor superfamily, PRLR signaling utilizes the JAK2/Stat pathways.[19–21]

We hypothesized that PRL may exert its immunomodulatory effects via alterations in T-bet expression and that PRLR-mediated signaling would involve JAK2/Stat pathways. Here, we test this hypothesis and its implications for the seemingly paradoxical effects of low- and high-dose PRL on immune response in $CD4^+$ T cells.

RESULTS

Prolactin-induced alterations in T-bet mRNA and protein expression use JAK2/Stat5 signaling

To address the effects of PRL on T-bet transcription, quantitative, real-time RT-PCR was used to assess T-bet mRNA levels in response to short-term exposure of $CD4^+$ T cells to PRL (Figure 1a). The expression of a PRLR in the $CD4^+$ T cells was confirmed by reverse transcription (RT)–PCR (data not shown). T-bet mRNA levels increased rapidly in the presence of low- and high-dose PRL. Although the alterations in T-bet transcription followed similar patterns, T-bet mRNA levels were higher with low-dose PRL exposure when compared to high-dose PRL exposure.

To ascertain the mechanism of transcriptional regulation involved in PRL-associated modulation of T-bet expression, we examined the PRL-induced phosphorylation of JAK2/Stat1 and 5, and correlated phosphorylation patterns with T-bet transcription levels (Figure 1b). Specific binding of phosphorylated Stat1 and 5 to the TRR was detected using oligonucleotide precipitation.[16] At baseline, TRR-bound phosphorylated Stat1 was present in $CD4^+$ cells, possibly as a result of stimulation by substances within the culture media. Low-dose PRL suppressed the phosphorylation of the TRR-bound Stat1 after 40 min of exposure, although an undulating pattern was noted at earlier time points. In contrast, TRR-bound phosphorylated Stat5a and 5b were barely detectable at baseline, but was rapidly induced by low-dose PRL exposure in $CD4^+$ cells. TRR-bound phosphorylated-Stat5 returned toward baseline levels by 40 min of exposure. These patterns were consistent with the alterations noted in T-bet mRNA levels upon low-dose PRL exposure (Figure 1a). The induction of JAK2 phosphorylation upon the low-dose PRL exposure mirrored that of TRR-bound phosphorylated Stat5a and 5b, suggesting that the JAK2/Stat5 pathway, rather than the JAK2/Stat1 pathway, is involved in PRL-associated alterations in T-bet expression.

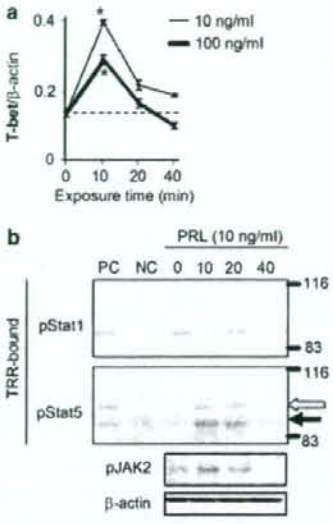

Figure 1 Prolactin (PRL) induces T-bet expression through the janus kinase 2 (JAK2)/signal transducers and activators of transcription 5 (Stat5) pathway. **(a)** $CD4^+$ T cells were exposed to PRL (10 or 100 ng ml^{-1}) for 10–40 min. mRNA was extracted from exposed cells and analyzed by quantitative RT-PCR using SYBR Green methodology. T-bet mRNA levels were normalized to β-actin. Regular and bold lines indicate 10 and 100 ng ml^{-1} of PRL exposures, respectively. Mean values with standard error bars are presented. Asterisks indicate those comparisons (vs basal levels: broken lines) with statistical significance ($P<0.05$). **(b)** $CD4^+$ T cells were exposed to low-dose PRL (10 ng ml^{-1}) for 10–40 min. Conjugated beads carrying oligonucleotides with the sequences of the T-bet regulatory region (TRR) were incubated with 100 μg of total cell extracts from pre-exposed or PRL-exposed cells. Extracts from $CD4^+$ T cells treated with interleukin (IL)-15, which induces phosphorylation of Stat1 and 5,[16,29] were incubated with TRR (positive control for phosphorylated Stat1 and 5) or mutTRR (negative control for sequence-specific binding to the TRR). Precipitants were denatured in sample buffer and separated across a 7.5% polyacrylamide gel. Anti-phosphorylated Stat1 (pY^{701}) or anti-phosphorylated Stat5 (pY^{694}) antibodies were used to immunoblot the precipitants. Molecular size markers of 116 and 83 kDa are shown on the right side of each panel. Open and closed arrows indicate the Stat5a (95 kDa) and 5b (91 kDa) forms, respectively. Cell extracts were separately resolved across an 8% polyacrylamide gel and anti-phosphorylated JAK2 ($pYpY^{1007/1008}$) and anti-β-actin antibodies were used for immunoblotting. β-Actin detection was added as an internal loading control.

PRLR signaling to the TRR is inhibited by SOCS1 and 3

We hypothesized that the dose dependence of prolactin's effects might involve negative regulators of JAK2/Stat5 signaling. Therefore, we investigated the dose-dependent effects of short-term PRL exposure on the synthesis and/or stability of factors that inhibit the JAK2/Stat pathway, the suppressors of cytokine signaling (SOCS) 1, SOCS3 and cytokine-inducible SH2-containing protein (CIS). In these experiments, we compared the alterations in the levels of inhibitory proteins with changes in the phosphorylation of JAK2 and TRR-bound Stat5 in $CD4^+$ T cells (Figure 2). PRL-associated increases in detectable SOCS1 and 3 were dose- and time dependent. PRL exposure also caused an increase in CIS protein levels; although this effect was neither dose- nor time dependent (at 10–100 ng ml^{-1} doses). Phosphorylation of JAK2 increased in a dose-dependent fashion upon exposure to low-dose PRL (10–30 ng ml^{-1}) but was reduced or returned to basal

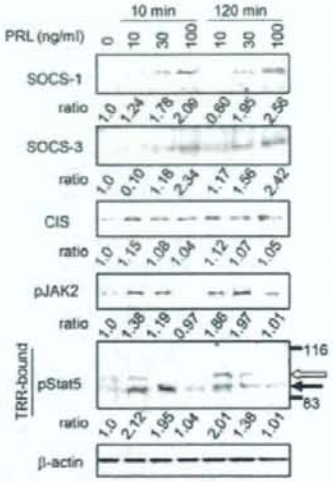

Figure 2 Prolactin (PRL) effects on negative regulators of the janus kinase (JAK)/signal transducers and activators of transcription (Stat) pathway. CD4+ T cells were exposed to PRL (10 or 100 ng ml^{-1}) for 10 or 120 min. Cell extracts from pre-exposed or PRL-exposed cells were separated across an 8 or 10% polyacrylamide gel. Anti-suppressors of cytokine signaling (SOCS)1, anti-SOCS3, anti-cytokine-inducible SH2-containing protein (CIS), anti-phosphorylated JAK2 (pYpY$^{1007/1008}$) and anti-β-actin antibodies were used for immunoblotting. For detection of T-bet regulatory region (TRR)-bound Stat5, oligonucleotide precipitation with the TRR was performed as described in Figure 2. The anti-phosphorylated Stat5 (pY^{694}) antibody was used to immunoblot the precipitants. Molecular size markers of 116 and 83 kDa are shown on the right side of the panel for Stat5. Open and closed arrows indicate the Stat5a (95 kDa) and 5b (91 kDa) forms, respectively. β-Actin detection was added as an internal loading control for cell extracts. Photodocumented immunoblot bands were quantitated using an image analyzer and normalized to β-actin. 'Ratio' refers to comparisons (exposure vs nonexposure) among normalized protein levels.

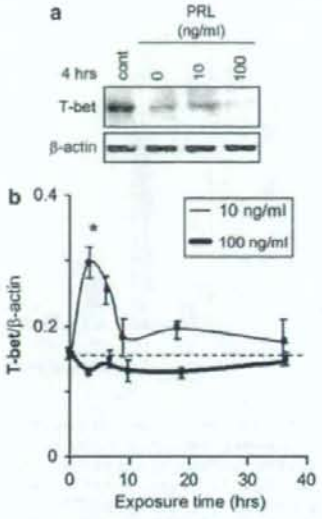

Figure 3 Dose-dependent effects of long-term prolactin (PRL) exposure on T-bet expression in CD4+ T cells. (a) CD4+ T cells were exposed to PRL (10 or 100 ng ml^{-1}) for 4 h. Nuclear extracts (50 μg) from exposed and control cells was separated over an 8% polyacrylamide gel and immunoblotted with a mouse anti-T-bet antibody (4B10) and a rabbit anti-β-actin antibody. Nuclear extracts from T-bet knockout mouse T cells that had been transduced with the murine T-bet gene were used as a positive control. Nuclear β-actin detection was added as an internal loading control for nuclear extracts. (b) CD4+ T cells were exposed to PRL (10 or 100 ng ml^{-1}) and harvested at 3, 6, 9, 18 or 36 h. mRNA was extracted from exposed cells and analyzed by quantitative RT-PCR using SYBR Green. T-bet (left) mRNA levels were normalized to β-actin. Fine and bold lines indicate 10 and 100 ng ml^{-1} of PRL exposures, respectively. Mean values with standard error bars are presented. Asterisks indicate those comparisons (vs basal levels; broken lines) with statistical significance ($P<0.05$).

levels with high-dose exposure (100 ng ml^{-1}). Phosphorylated JAK2 levels were similar after 10 and 120 min of exposure, so time dependence was minimal. Like the alterations in phosphorylated JAK2, the levels of TRR-bound phosphorylated Stat5 increased after exposure to 10–30 ng ml^{-1} of PRL but were reduced or unaltered in the presence of 100 ng ml^{-1} of PRL. TRR-bound phosphorylated Stat1 was not altered with PRL dose escalation (data not shown).

Dose-dependent differences in the effects of PRL on T-bet expression are magnified with long-term exposures

T-bet expression was induced by low-dose short-term PRL exposure and signaling appeared to involve the JAK2/Stat5 pathway. To more thoroughly address the described paradoxical effects of low- and high-dose PRL on immune function, we performed similar experiments using longer PRL exposure times (Figure 3). Western immunoblotting of nuclear extracts from CD4+ T cells demonstrated that the cells express T-bet protein (Figure 3a). Low-dose PRL (10 ng ml^{-1}) exposure for 4 h increased T-bet protein levels, whereas high-dose PRL (100 ng ml^{-1}) suppressed it slightly. In the CD4+ T cell line, low-dose PRL exposure again induced T-bet mRNA production, peaking at 3 h and returning toward baseline levels by 9 h (Figure 3b). High-dose PRL exposure of CD4+ T cells suppressed T-bet transcription throughout the entire 36 h. In summary, long-term, low-dose PRL induced T-bet, whereas high-dose PRL suppressed T-bet transcription.

Rodent T cells have been known to respond to human PRL through the PRLR.[20,21] Primary CD4+ T cells were obtained from nonlactating female mice and examined to see if the PRL effects on T-bet transcription occurred in a dose-dependent manner. Murine primary CD4+ T cells were isolated from mice spleens using positive selection by magnetic beads bearing anti-CD4 monoclonal antibodies (mAbs). Primary CD4+ T cells were exposed to human PRL in culture medium at concentrations of 0, 10, 30 or 100 ng ml^{-1} for 3 h and then examined for alterations in T-bet mRNA levels (Figure 4). Low-dose PRL (10 ng ml^{-1}) dramatically increased T-bet mRNA levels in CD4+ primary T cells. The increased T-bet mRNA levels were much higher in primary CD4+ T cells than the CD4+ T cell line shown in Figure 3, although the basal levels were equivalent for both. T-bet mRNA levels decreased with dose escalation and were below unexposed levels in the presence of 100 ng ml^{-1} of PRL. In primary CD4+ T cells, high-dose PRL (100 ng ml^{-1}) tended to suppress T-bet expression, although the difference between basal and high-dose PRL-exposed T-bet levels was not significant ($P=0.077$).

DISCUSSION

We have approached the paradoxical dose-dependent effects of prolactin on immune function by investigating the modulation of T-bet promoter activity and T-bet production upon exposure to low- and high-dose PRL. PRL-associated alterations in T-bet

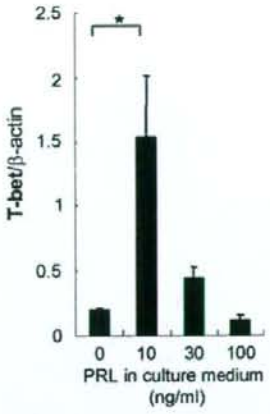

Figure 4 Dose-dependent effects of long-term prolactin (PRL) exposure on T-bet expression in primary CD4+ T cells. Nonlactating female Balb/c mice (60-day old) were killed and their spleens were removed and homogenized in culture medium. CD4+ T cells were purified from splenocyte by positive selection using magnetic beads bearing anti-CD4 monoclonal antibodies (mAbs). The isolated primary CD4+ T cells were exposed to human PRL at several concentrations (10, 30 or 100 ng ml^{-1}) for 3 h. mRNA was extracted from nonexposed or exposed cells and analyzed by quantitative RT-PCR using SYBR Green. T-bet mRNA levels were normalized to β-actin. Mean values with standard error bars are presented. Asterisks indicate those comparisons (vs nonexposure) with statistical significance ($P<0.05$).

expression paralleled those in the JAK2/Stat5 pathway, rather than the JAK2/Stat1 pathway, in both time- and dose-dependent manners. We propose a possible mechanism for dose-dependent alterations of T-bet expression that depends upon the balance of PRL/JAK2/Stat5 and PRL/SOCS1 and 3 signaling pathways. The induction of T-bet expression in the presence of low-dose PRL has an undulating pattern over time.

We have previously shown that upregulation of T-bet expression associated with hormone exposure is mediated by JAK2/Stat5 signaling, followed by the binding of phosphorylated Stat5 to a GAS element in the TRR.[16] Although Stat protein activity is characteristically mediated by binding to a given promoter at the site of a GAS element, the PRL-induced action of Stat proteins on gene expression differs depending on the target gene and the PRL dosage. In T cells, it has been shown that PRL-induced Stat1 and Stat5 act as dose-dependent activators of the β-casein promoter.[21] Using the JAK2/Stat5 pathway, PRL also induces glycosylation-dependent cell adhesion molecule promoter activity in a dose-dependent fashion.[22] In primary endometrial glandular cells, PRL (100 ng ml^{-1}) rapidly induces the phosphorylation of JAK2/Stat proteins (within 20 min after exposure).[9] Finally, dose-dependent and opposing effects of PRL on IRF-1 expression in T cells have been associated with alterations in Stat protein-mediated signaling.[7,8] In this system, high-dose PRL inhibits the IRF-1 promoter via Stat5, but low-dose PRL induces IRF-1 through Stat1.

In contrast to the Stat protein-mediated suppression of IRF-1 by high-dose PRL, the inhibition of T-bet expression appears to be mediated by the inhibitory effects of SOCS1 and SOCS3. Both suppressors are increased in response to high-dose PRL exposure. SOCS1, SOCS3 and CIS are known to inhibit JAK/Stat signaling and thereby impair a diverse array of immunologic activities.[23] SOCS1 and 3 directly bind to the kinase domains of JAK proteins and inhibit their tyrosine kinase activity.[23,24] CIS binds to cytokine receptors and inhibits the recruitment of Stat5 by the receptors.[24] In PRLR signaling, SOCS1 and 3 inhibit the PRLR/JAK2/Stat5 pathway in a PRL dose-dependent manner by binding of SOCS1 to JAK2 proteins and SOCS3 to PRLR.[25–28] SOCS1 and 3 increase rapidly in response to PRL signaling and switch off PRLR/JAK2/Stat5 signaling.[26] Anderson *et al.*[28] recently reported that treatment of nonpregnant female rat with prolactin increases levels of SOCS1 and 3 in a PRL dose-dependent manner. In late pregnant and lactating rats, PRL loses the ability to activate Stat5b and this is associated with an increase in SOCS1 and 3. CIS binds to PRLR as well as to conventional cytokine receptors, but its inhibitory actions on the PRLR/Stat5 pathway appear to differ depending on the experimental promoter activity assessed.[25,26] In our study, the increase in the detectable amounts of CIS in response to PRL was independent of PRL dose, and this effect was not correlated with alterations in the phosphorylation of TRR-bound Stat5. In turn, the levels of SOCS1 and 3 were negatively correlated with phosphorylation of JAK2 and TRR-bound Stat5. To summarize, we show that SOCS1 and 3, but not CIS, appear to inhibit signaling of T-bet gene expression via the PRLR/Stat5 pathway in a PRL-dose-dependent manner.[25–27] This may explain the divergent effects of low- and high-dose prolactin on T-bet expression and downstream immune responses.

In low-dose PRL exposure, T-bet mRNA levels peaked rapidly at 10 min of exposure, returned toward baseline levels by 40 min of exposure and then rose again at 3 h of exposure as shown in Figures 1 and 3. This suggests that T-bet expression is modulated by PRLR-mediated signaling in an undulating fashion. Indeed, low-dose PRL is reported to promote a similar induction pattern for IRF-1 expression.[7] Since alterations in SOCS1 and 3 expression in the presence of low-dose PRL were minimal, undulations in T-bet expression may result from a suppression of the JAK2/Stat5 pathway by cellular inhibitory factors in response to PRL signaling rather than SOCS molecules.

The PRL effects on T-bet expression were observed in not only CD4+ T cell line but also in murine primary CD4+ T cells. This clearly confirms that low-dose PRL induce T-bet expression in CD4+ T cells, whereas high-dose PRL suppresses it. The noted induction in T-bet mRNA levels was much higher in murine primary CD4+ T cells than in the human CD4+ T cell line. The difference between the human cell line and murine primary cells might be the result of T-bet polymorphisms or differences in responsivity within PRLR-mediated intracellular pathways. Alternatively, the primary CD4+ T cells used may include many Th1-differentiated cells producing IFN-γ, which in turn induces T-bet expression.

How does PRL-regulated T-bet act on the immune system? T-bet promotes IFN-γ secretion from naive CD4+ T cell and DCs forming a positive feedback loop that enhances the Th1 environment.[11–15] We have previously demonstrated that T-bet can induce IL-15 production in EECs and have hypothesized that the IL-15/T-bet/IL-15 pathway may allow positive feedback support to the Th1 microenvironment within mucosal epithelia.[16] In CD4+ T cells, low-dose PRL induced, but high-dose PRL suppressed, T-bet expression; an effect that was rapid but transient. Low-dose PRL (10–30 ng ml^{-1}) promotes the secretion of Th1-type cytokines (IFN-γ, IL-12) from human whole blood, whereas high-dose PRL (more than 100 ng ml^{-1}) has little effect.[10] In conjunction with data presented here, this suggests that low-dose PRL promotes systemic Th1-type cytokine secretion through increases in T-bet, whereas high-dose PRL has mildly suppressive effects. High and sustained levels of PRL, such as those existing in pregnancy, may synergize with female steroid hormones to protect the embryo from local and systemic maternal Th1 and innate immune responses.

METHODS

Cell line and cytokine/hormone exposure

8E5 cells are a $CD4^+$ T cell line derived from a human T-cell leukemia that expresses human immunodeficiency virus structural proteins (American Type Culture Collection, Manassas, VA, USA). 8E5 cells were cultured in RPMI 1640 (Invitrogen Corporation, Carlsbad, CA, USA) supplemented with 10% fetal calf serum and penicillin/streptomycin (Invitrogen Corporation). The cells were exposed to human PRL (Sigma-Aldrich Inc., St Louis, MO, USA) at several concentrations (10, 30 or 100 ng ml^{-1}) for times ranging from 10 min to 36 h. Cells were harvested at 10, 20 or 40 min time points for short-term exposures and 3, 6, 9, 18 or 36 h time points for long-term exposures.

Exposure of murine primary $CD4^+$ T cells to prolactin

Nonlactating female Balb/c mice (60-day old) were killed and their spleens were removed and homogenized in RPMI 1640 (Invitrogen Corporation) supplemented with 10% fetal calf serum and penicillin/streptomycin (Invitrogen Corporation). Anti-CD4 mAb (1 µg ml^{-1}; Dako, Kyoto, Japan) was mixed with 2×10^8 magnetic beads (Dynabeads; CellectionTM PanMouse IgG Kit; Dynal Biotech, Oslo, Norway) in 10 ml of phosphate-buffered saline (PBS) with 0.1% bovine serum albumin (BSA) and was incubated for 3 h at room temperature. For purification of $CD4^+$ T cells, we used positive selection by magnetic beads bearing anti-CD4 mAbs. A total of 1×10^7 antibody-coated magnetic beads were incubated with 2×10^6 splenocytes suspended in 1 ml of PBS with 0.1% BSA for 30 min at 4 °C with gentle agitation. The cells attached to the beads were removed using a magnetic collector and incubated in RPMI medium for 3 h before PRL exposure. Isolated $CD4^+$ T cells were then exposed to human PRL (Sigma-Aldrich Inc.) at several concentrations (0, 10, 30 or 100 ng ml^{-1}) for 3 h in RPMI medium.

Real-time PCR

For quantitative analyses, mRNA from exposed and nonexposed 8E5 cells, or murine primary $CD4^+$ T cells, were subjected to real-time RT-PCR using 1 µg of total RNA. Human T-bet and β-actin RNA expression levels were assessed using SYBR Green (Qiagen Inc., Valencia, CA, USA) methodology. In these experiments, the following primer pairs amplified a single PCR product for each gene: T-bet (67 bp): forward 5′-AACCGCCTGTACGTCCACC-3′, reverse 5′-ATGAAACTTCCTGGCGCATC-3′; β-actin (113 bp): forward 5′-GAAA TCGTGCGTGACATTAAGG-3′, reverse 5′-TCAGGCAGCTCGTAGCTTCT-3′. The mRNA levels of T-bet were normalized to those of β-actin.

Western immunoblotting

Treated and control 8E5 cells were harvested and 50 µg of nuclear extracts[16] was used for western immunoblotting. Protein concentrations were measured using standard protein assay kits (Pierce Biotechnology, Rockford, IL, USA). Using the 4B10 mAb (Santa Cruz Biotechnology Inc., Santa Cruz, CA, USA) in standard western immunoblotting, a T-bet-specific band was observed at 62 kDa on an 8% polyacrylamide gel. Nuclear extracts from T-bet knockout mouse T cells transduced with the murine T-bet gene (kind gift from Dr LH Glimcher, Harvard School of Public Health, Boston, MA, USA) were used as a positive control. As loading controls for nuclear extracts, nuclear β-actin proteins were detected by western immunoblotting using a rabbit anti-β-actin polyclonal antibody (1:1000; Abcam Inc., Cambridge, MA, USA).

For experiments involving the detection of the SOCS1 and 3, the CIS and phosphorylated JAK2, 8E5 $CD4^+$ T cells with or without PRL exposure were lysed in lysis buffer (1% NP-40, 10% glycerol, 10 mM 4-(2-hydroxyethyl)-1-piperazineethanesulfonic acid, 150 mM KCl, 2 mM EDTA, 1 mM ethylene glycol tetraacetic acid (EGTA), 0.5 mM dithiothreitol (DTT), 1 mM Na_3VO_4 and protease inhibitors (Sigma-Aldrich Inc.)) and 50 µg of total cell lysates separated on an 8% polyacrylamide gel. Separated proteins were transferred to a polyvinylidene fluoride membrane and immunoblotted with anti-SOCS1 and 3 (1:400; Santa Cruz Biotechnology Inc.), anti-CIS (1:400; Abcam Inc.) or anti-phosphorylated JAK2 ($pYpY^{1007/1008}$) antibodies (1:400; Biosource International Inc., Carlsbad, CA, USA). The molecular weight of the band corresponding to phosphorylated JAK2 was confirmed by comparison to standard molecular weight markers and molecular weight analysis (FluorChem SP Alpha Innotech, San Leandro, CA, USA). Photodocumented immunoblot bands were analyzed using image analysis software (Scion Image, Frederick, MD, USA) and normalized to β-actin.

Oligonucleotide precipitation

A putative binding site for Stat family members was identified in the TRR by the presence of an IFN GAS element, $TTC(N)_4GAA$, at 1200 bp from the T-bet gene.[16] Three nucleotides in the core motif of this GAS element were replaced with alternative nucleotides to serve as a negative control (NC) for oligonucleotide precipitations. Biotinylated 50-mer oligonucleotides with sequences derived from the TRR (5′-biotin-TTGAACTATATCCCAGACCCCGGGG ATGCTTTTTATTTCAAAAGAAAACT-3′) or mutTRR (5′-biotin-TTGAACT ATATCCCAGACCCCGGGGATGCTTTTTATTaCAAActAAAACT-3′) were synthesized (Invitrogen Corporation) and streptavidin bead-conjugated (Pierce Biotechnology) for precipitation. Total cell extracts from pre-exposed or PRL-exposed cells were prepared in lysis buffer with 2 mM EDTA, 1 mM EGTA, 0.5 mM DTT, 1 mM Na_3VO_4 and protease inhibitors (Sigma-Aldrich Inc.). Protein concentrations were measured using standard protein assay kits (Pierce Biotechnology). Conjugated beads carrying 25 pmol of oligonucleotides with the sequences of either the TRR were incubated with 100 µg of total cell extracts for 4 h at 4 °C in binding buffer.[16] Extracts from $CD4^+$ T cells exposed to IL-15 as described previously,[16] which induces phosphorylation of Stat1 and 5,[16,29] were incubated with TRR as a positive control for phosphorylated Stat1 and 5 or with mutTRR (NC). Precipitants were boiled in sample buffer for 5 min and separated over a 7.5% polyacrylamide gel.

Anti-phosphorylated Stat1 (pY^{701}) (Biosource International Inc.) or anti-phosphorylated Stat5 (pY^{694}) antibodies (Santa Cruz Biotechnology Inc.) were used at 1:500 working concentration for western immunoblotting of precipitants. β-Actin proteins were detected by western immunoblotting using a rabbit anti-β-actin polyclonal antibody (Abcam Inc.) (1:1000) and served as an internal control. The molecular weight of each band corresponding to a Stat protein was confirmed by comparison to standard molecular weight markers and molecular weight analysis (FluorChem SP Alpha Innotech).

Statistical analysis

T-bet mRNA levels from PRL-exposed cells were compared to pre-exposure levels using standard analysis of variance or Student's *t*-testing. A *P*-value of <0.05 was considered significant.

ACKNOWLEDGEMENTS

We are grateful to Dr Eun Sook Wang for her kind gift of a positive control for the T-bet protein, and to Dr LS Graziadei and CD McGahan for editorial assistance.

1 Reber PM. Prolactin and immunomodulation. *Am J Med* 1993; **5**: 637–644.
2 Gala RR. Prolactin and growth hormone in the regulation of the immune system. *Proc Soc Exp Biol Med* 1991; **198**: 513–527.
3 Yu-Lee LY, Luo G, Book ML, Morris SM. Lactogenic hormone signal transduction. *Biol Reprod* 1998; **58**: 295–301.
4 Bouchard B, Ormandy CJ, Di Santo JP, Kelly PA. Immune system development and function in prolactin receptor-deficient mice. *J Immunol* 1999; **163**: 576–582.
5 Golander A, Hurley T, Barrett J, Hizi A, Handwerger S. Prolactin synthesis by human chorion-decidual tissue: a possible source of prolactin in the amniotic fluid. *Science* 1978; **202**: 311–313.
6 Tyson JE, Hwang P, Guyda H, Friesen HG. Studies of prolactin secretion in human pregnancy. *Am J Obstet Gynecol* 1972; **113**: 14–20.
7 Stevens AM, Wang YF, Sieger KA, Lu HF, Yu-Lee LY. Biphasic transcriptional regulation of the interferon regulatory factor-1 gene by prolactin: involvement of gamma-interferon-activated sequence and Stat-related proteins. *Mol Endocrinol* 1995; **9**: 513–525.
8 Luo G, Yu-Lee L. Transcriptional inhibition by Stat5. Differential activities at growth-related versus differentiation-specific promoters. *J Biol Chem* 1997; **272**: 26841–26849.
9 Jabbour HN, Critchley HO, Yu-Lee LY, Boddy SC. Localization of interferon regulatory factor-1 (IRF-1) in nonpregnant human endometrium: expression of IRF-1 is up-regulated by prolactin during the secretory phase of the menstrual cycle. *J Clin Endocrinol Metab* 1999; **84**: 4260–4265.

10 Matalka KZ. Prolactin enhances production of interferon-gamma, interleukin-12, and interleukin-10, but not of tumor necrosis factor-alpha, in a stimulus-specific manner. *Cytokine* 2003; **21**: 187–194.
11 Szabo SJ, Kim ST, Costa GL, Zhang X, Fathman CG, Glimcher LH. A novel transcription factor, T-bet, directs Th1 lineage commitment. *Cell* 2000; **100**: 655–669.
12 Robinson DS, O'Garra A. Further checkpoints in Th1 development. *Immunity* 2002; **16**: 755–758.
13 Hwang ES, Szabo SJ, Schwartzberg PL, Glimcher LH. T helper cell fate specified by kinase-mediated interaction of T-bet with GATA-3. *Science* 2005; **307**: 430–433.
14 Lighvani AA, Frucht DM, Jankovic D, Yamane H, Aliberti J, Hissong BD *et al*. T-bet is rapidly induced by interferon-gamma in lymphoid and myeloid cells. *Proc Natl Acad Sci USA* 2001; **98**: 15137–15142.
15 Lugo-Villarino G, Maldonado-Lopez R, Possemato R, Penaranda C, Glimcher LH. T-bet is required for optimal production of IFN-gamma and antigen-specific T cell activation by dendritic cells. *Proc Natl Acad Sci USA* 2003; **100**: 7749–7754.
16 Kawana K, Kawana Y, Schust DJ. Female steroid hormones utilize Stat protein-mediated pathways to modulate the expression of T-bet in epithelial cells: a mechanism for local immune regulation in the human reproductive tract. *Mol Endocrinol* 2005; **19**: 2047–2059.
17 Kamiya S, Owaki T, Morishima N, Fukai F, Mizuguchi J, Yoshimoto T. An indispensable role for STAT1 in IL-27-induced T-bet expression but not proliferation of naive CD4$^+$ T cells. *J Immunol* 2004; **173**: 3871–3877.
18 Gagnerault MC, Touraine P, Savino W, Kelly PA, Dardenne M. Expression of prolactin receptors in murine lymphoid cells in normal and autoimmune situations. *J Immunol* 1993; **150**: 5673–5681.
19 Leonard WJ, O'Shea JJ. Jaks and STATs: biological implications. *Annu Rev Immunol* 1998; **16**: 293–322.
20 Murphy WJ, Durum SK, Anver MR, Longo DL. Immunological and haematological effects of neuroendocrine hormone: studies on DW/J dwarf mice. *J Immunol* 1992; **148**: 3799–3808.
21 Gouilleux F, Moritz D, Humar M, Moriggl R, Berchtold S, Groner B. Prolactin and interleukin-2 receptors in T lymphocytes signal through a MGF-STAT5-like transcription factor. *Endocrinology* 1995; **136**: 5700–5708.
22 Hou Z, Srivastava S, Mistry MJ, Herbst MP, Bailey JP, Horseman ND. Two tandemly linked interferon-gamma-activated sequence elements in the promoter of glycosylation-dependent cell adhesion molecule 1 gene synergistically respond to prolactin in mouse mammary epithelial cells. *Mol Endocrinol* 2003; **17**: 1910–1920.
23 Alexander WS, Hilton DJ. The role of suppressors of cytokine signaling (SOCS) proteins in regulation of the immune response. *Annu Rev Immunol* 2004; **22**: 503–529.
24 Yasukawa H, Sasaki A, Yoshimura A. Negative regulation of cytokine signaling pathways. *Annu Rev Immunol* 2000; **18**: 143–164.
25 Dif F, Saunier E, Demeneix B, Kelly PA, Edery M. Cytokine-inducible SH2-containing protein suppresses PRL signaling by binding the PRL receptor. *Endocrinology* 2001; **142**: 5286–5293.
26 Pezet A, Favre H, Kelly PA, Edery M. Inhibition and restoration of prolactin signal transduction by suppressors of cytokine signaling. *J Biol Chem* 1999; **274**: 24497–24502.
27 Ali S, Nouhi Z, Chughtai N, Ali S. SHP-2 regulates SOCS-1-mediated Janus kinase-2 ubiquitination/degradation downstream of the prolactin receptor. *J Biol Chem* 2003; **278**: 52021–52031.
28 Anderson GM, Beijer P, Bang AS, Fenwick MA, Bunn SJ, Grattan DR. Suppression of prolactin-induced signal transducer and activator of transcription 5b signaling and induction of suppressors of cytokine signaling messenger ribonucleic acid in the hypothalamic arcuate nucleus of the rat during late pregnancy and lactation. *Endocrinology* 2006; **147**: 4996–5005.
29 Strengell M, Matikainen S, Sirén J, Lehtonen A, Foster D, Julkunen I *et al*. IL-21 in synergy with IL-15 or IL-18 enhances IFN-gamma production in human NK and T cells. *J Immunol* 2003; **170**: 5464–5469.

JOURNAL OF VIROLOGY, Sept. 2008, p. 8820–8827 Vol. 82, No. 17
0022-538X/08/$08.00+0 doi:10.1128/JVI.02363-07

Ras Modifies Proliferation and Invasiveness of Cells Expressing Human Papillomavirus Oncoproteins▽

Satoshi Yoshida, Naoko Kajitani, Ayano Satsuka, Hiroyasu Nakamura, and Hiroyuki Sakai*

Laboratory of Gene Analysis, Department of Viral Oncology, Institute for Virus Research, Kyoto University, Sakyo-ku, Kyoto 606-8507, Japan

Received 1 November 2007/Accepted 19 June 2008

Infection by human papillomavirus (HPV) is a major risk factor for human cervical carcinoma. However, the HPV infection alone is not sufficient for cancer formation. Cervical carcinogenesis is considered a multistep process accompanied by genetic alterations of the cell. Ras is activated in approximately 20% of human cancers, and it is related to the metastatic conversion of tumor cells. We investigated how Ras activation was involved in the malignant conversion of HPV-infected lesions. The active form of H-ras was introduced into human primary keratinocytes expressing the HPV type 18 (HPV18) oncoproteins E6 and/or E7. We analyzed the keratinocytes' growth potentials and found that the activation of the Ras pathway induced senescence-like growth arrest. Senescence could be eliminated by high-risk E7 expression, suggesting that the pRb pathway was important for Ras-induced senescence. Then we analyzed the effect of Ras activation on epidermis development by using an organotypic "raft" culture and found that the E7 and H-ras coexpressions conferred invasive potential on the epidermis. This invasiveness resulted from the upregulation of MT1-MMP and MMP9 by H-ras and E7, respectively, in which the activation of the MEK/extracellular signal-regulated kinase pathway was involved. These results indicated that the activation of Ras or the related signal pathways promoted the malignant conversion of HPV-infected cells.

It has been proposed that carcinogenesis is a multistep process accompanied by multiple genetic alterations (4, 55). Hyperplasia is considered the first step of carcinogenesis, which is induced by inflammation, activation of growth signals, or organ regeneration. Among the expanding population of cells, some cells acquire genetic mutations in the genes that regulate cell division, motility, and invasiveness. If the mutation disrupts the cell cycle checkpoint machinery, genetic instability is induced, resulting in the acceleration of genetic alterations. Immortalization can be induced by reactivation of telomerase and/or disruption of the pRb pathway. These multiple processes are required for the malignant conversion of the cell.

Cervical cancer is one of the gynecological cancers. Human papillomaviruses (HPVs) are detected in more than 90% of cervical cancer cases (59), and HPV infection is considered a major causative factor for the cancer. HPVs are small DNA viruses which have about 8,000-bp, double-strand DNA as the genome (25). More than 100 types of HPVs have been reported (59), which are classified as low-risk and high-risk types according to their associations with malignant tumors (59). High-risk HPVs encode two oncogenes, E6 and E7, which play important roles in carcinogenesis (36). E6 has two zinc finger domains and interacts with tumor suppressor p53 (7) and degrades it to escape from apoptosis and to disrupt cell cycle checkpoint machinery (45). E7 interacts with the tumor suppressor pRb and degrades or inactivates it to escape from the checkpoint machinery and to induce genome instability (11, 12). Although the inactivation of both p53 and pRb seems to be pivotal for oncogenesis by HPV, other functions of these oncoproteins also contribute to carcinogenesis. E6 is able to reactivate human telomerase activity, resulting in immortalization of the infected cell (29). E6 has a PDZ-binding domain at the C terminus that interacts with PDZ proteins (32), such as hDlg and hScrib, the association of which is reported to be involved in the transformation function (28, 38). E7 inactivates Cdk inhibitor p21 and disrupts the cell cycle checkpoint (23, 27) and enhances *myc* expression to upregulate cell proliferation (40, 41).

Although HPV infection is critical for cervical oncogenesis, most infected lesions do not proceed to the malignant tumor stage, and a long incubation period is required for cancer development (14, 46), indicating that HPV infection alone is not sufficient and that several genetic alterations of the cell are required for the induction of cervical cancer. Even though many mutations have been reported for HPV-positive cervical cancer (54), the critical genes responsible for cancer development have not been identified.

ras is a proto-oncogene which is frequently mutated or amplified in human cancers (3). Activating types of *ras* mutations are detected in approximately 20% of all human cancers (10). Ras regulates cell proliferation and migration through the activation of mitogen-activated protein kinase (MAPK), phosphatidylinositol 3-kinase, and the Rac/Rho signaling pathways (48). *ras* mutation and amplification have also been detected in some cases of cervical cancers, and the involvement of Ras activation in HPV-induced carcinogenesis was proposed by several reports (2, 44). Ras activation upregulated the gene expression levels of E6 and E7 (34). Ras was reported to contribute to cellular transformation in cooperation with E6 and E7 in the mouse model (19, 47). With clinical samples, the

* Corresponding author. Mailing address: Laboratory of Gene Analysis, Department of Viral Oncology, Institute for Virus Research, Kyoto University, 53 Kawahara-cho, Sakyo-ku, Kyoto 606-8507, Japan. Phone: 81-75-751-3996. Fax: 81-75-751-4010. E-mail: hsakai@virus.kyoto-u.ac.jp.

▽ Published ahead of print on 25 June 2008.

rate of *ras* mutation was reported to increase in association with the lesion's grade of cervical neoplasia (2). These findings suggested that Ras activation is one of the major genetic alterations in the development of cervical cancer.

To clarify HPV-induced carcinogenesis and to prevent cancer progression, an understanding of the HPV life cycle is essential. It is known that HPV replication has an intimate connection with the differentiation process of keratinocytes (39, 56). Virion production is restricted in the differentiated layer of epidermis; therefore, the standard monolayer culture of keratinocytes is unable to support the HPV life cycle. To analyze virion production, a culture medium containing a high concentration of calcium ions (15) or a suspension culture with semisolid medium (43) has been employed, by which some aspects of viral replication have been studied. An organotypic raft culture is one of the culture systems used for studying viral replication, which can reproduce an epidermal structure in vitro and support the whole life cycle of HPV (9, 35). It seems better to use the culture condition that can support HPV replication for evaluating viral gene functions and for analyzing virus-induced oncogenesis because some of these aspects might be cell and/or tissue specific.

In this report, we analyzed the effects of Ras activation on HPV-induced tumorigenesis, using human primary keratinocytes. Studies of the transformation activity of Ras were performed mainly with rodent fibroblasts and mouse model systems. As noted above, however, it is important to use the assay system suitable for studying the HPV life cycle. We employed the organotypic raft culture and found functions of E7 and Ras that cooperated in the acquisition of invasiveness. We also found that the induction of matrix metalloproteases (MMPs) by E7 and H-ras was involved in invasiveness. These observations indicated that the activation of Ras or the related pathways conferred invasive potential on HPV-infected cells.

MATERIALS AND METHODS

Vector constructions. HPV oncogenes (E6 and E7) were isolated by PCR with a full-length HPV type 18 (HPV18) clone (GenBank accession number X05015) as the template and then inserted into the pLXSN (BD Biosciences Clontech, Palo Alto, CA; GenBank accession number M28248) vector. The active form of the human H-ras (G12V) gene, which was inserted into the pMXpuro vector with a hemagglutinin tag at the N terminus, was provided by Ishikawa (Laboratory of Cell Cycle Regulation, Dept. of Gene Mechanisms, Div. of Integrated Life Science, Graduate School of Biostudies, Kyoto University, Japan). The DNA fragment containing the H-ras sequence was isolated by EcoRI and then cut by BglII. The fragment was inserted into the pLPCX (BD Biosciences Clontech, Palo Alto, CA) vector. MAPK constitutive active mutants (*mek1*-SDSE [*Xenopus*, S218D, S222E], *mkk7*-DED [mouse, S287D, T291E, S293D], and *mkk6*-SETE [human, S207E, T211E]) (21) were provided by Nishida (Laboratory of Signal Transduction, Dept. of Cell and Developmental Biology, Div. of Integrated Life Science, Graduate School of Biostudies, Kyoto University, Japan). The DNAs encoding these MAPK mutants were amplified by PCR and then inserted into pLPCX. The short hairpin RNA (shRNA) sequences used for pRb were GAT ACT AGA TCG TGT CAG ATT CAA GAG ATC TGA CAT GAT CTG GTA TCT TTT TTA TCG AT. The annealed oligonucleotides were inserted into the pSIREN-RetroQ vector (BD Biosciences Clontech, Palo Alto, CA).

Cell cultures. Human foreskin keratinocytes (HFKs; Kurabo Industries, Ltd., Osaka, Japan) were maintained with serum-free keratinocyte growth medium (KGM; product, EpiLife-KG2; Kurabo). Human foreskin fibroblasts (HFFs; Kurabo), HeLa cells, and 293T cells were maintained with Dulbecco's modified minimal essential medium (DMEM) supplemented with 10% fetal bovine serum (growth medium).

Retroviral production and infection. 293T cells were transfected with the retroviral gene expression plasmid (3.5 μg: pLXSN or pLPCX), pCL10A1 (1 μg; Imgenex Corp., San Diego, CA), and pGreenLantern-1 (0.5 μg; Invitrogen Corp., Carlsbad, CA) and herring sperm DNA (5 μg; Roche Diagnostics, GmbH, Mannheim, Germany) by using the calcium phosphate coprecipitation method. At day 2 after transfection, the culture medium was replaced with fresh KGM, and the retroviral vector was collected in the medium for 8 h. The conditioned medium containing viral vector was clarified through a 0.45-μm-pore filter and used for the infection of HFKs. For the infection procedure, the previous KGM was removed, and the virus-containing medium mixed with 8 μg/ml polybrene was overlaid on the HFKs. The cells were maintained for 6 h in a CO_2 incubator, and then the medium was changed to fresh KGM. At 24 h after infection, the cells were spread at a low density. G418 (60 μg/ml) and puromycin (0.2 μg/ml) were added to the medium at 48 h after infection, and the cells were incubated for 4 to 7 days.

SA-β-gal assay. H-ras and HPV oncoprotein-coexpressing HFKs were spread at 1.0×10^5 cells/dish. After 24 h, an evaluation of senescence was performed with a senescence-associated β-galactosidase (SA-β-gal) assay kit (Cell Signaling Technology, Inc., Danvers, MA) by following the manufacture's instructions.

Immunoblot analysis. Total cell lysates were prepared with triple-detergent lysis buffer (50 mM Tris HCl [pH 8.0], 150 mM NaCl, 0.1% sodium dodecyl sulfate [SDS], 1% Nonidet P-40, 0.5% sodium deoxycholate) supplemented with protease inhibitor cocktail (Nakarai Tesque, Kyoto, Japan). The cell lysates were subjected to SDS-polyacrylamide gel electrophoresis, and immunoblot analysis was performed by using a standard protocol. The antibodies used in the experiment were anti-18-E7 (clone C-20), anti-H-Ras (clone 259) (Santa Cruz Biotechnology, Inc., Santa Cruz, CA), and an pRb-specific antibody (BD Biosciences Pharmingen, San Diego, CA).

Organotypic raft culture. For a preparation of the dermal equivalent, one part type I collagen (cell matrix type I-P; Nitta Gelatin Co., Ltd., Osaka, Japan) and two parts growth medium containing HFFs (1×10^6 cells) were mixed while they cooled and were poured into a 6-cm dish, and then the cells were maintained in a 5% CO_2 incubator at 37°C until the collagen gel contracted to about a 2-cm diameter. The gel was soaked in fresh KGM for several hours and then transferred in a Transwell insert. The gel was put in a 6-well plate, and fresh KGM was filled into both the bottom and the insert. HFKs were overlaid on the gel (day 0). At day 1, the medium was changed to a mixture of KGM and DMEM growth medium (KGM/DMEM, 1:1), and 24 h later, the medium was changed to the same mixture, adjusting the $CaCl_2$ concentration to 1.8 mM (day 2). On day 3, the surface of the collagen gel was exposed to air, and then the medium in the bottom was changed to fresh medium every day. Multilayered cultures of keratinocytes were obtained at day 10.

The construction of the raft culture with HeLa cells was performed by a protocol similar to that described above, except that DMEM supplemented with 10% fetal bovine serum was used for the HeLa cells.

Hematoxylin and eosin (H&E) staining. Specimens of raft culture were embedded in optimal cutting temperature compound (Sakura Finetechnical Co., Ltd., Tokyo, Japan), and thin sections (7 μm) were obtained by cryosectioning (Cryo-Star HM560M machine; Microm Laborgeräte GmbH, Walldrof, Germany). The sections were transferred onto slide glasses and dried. They were stained with hematoxylin 3G (Sakura) for 5 min. After sections were washed with water, they were rinsed with HCl (4×10^{-3} N) for about 1 min and washed again. They were then stained with a pure eosin solution (Sakura) for 3 min and destained with 80% ethanol.

Immunohistochemical analysis. The cryosections were fixed with Mildform 10N (Wako Pure Chemical Industries, Ltd., Osaka, Japan) and then treated with a target retrieval solution (Dako Japan KK, Kyoto, Japan). The endogenous peroxidase activity was quenched with 0.3% H_2O_2-MeOH after the target retrieval process. Antigen detection was performed with a tyramide signal amplification-biotin system (Perkin-Elmer, Boston, MA) by following the manufacture's instructions. Chromogenic detection of horseradish peroxidase was performed with a Metal Enhanced 3,3'-diaminobenzidine substrate kit (Pierce Biotechnology, Rockford, IL). Antibodies for MMP2, MMP9, and MT1-MMP (Daiichi Fine Chemical Co., Ltd., Toyama, Japan) and a secondary antibody for mouse (Santa Cruz Biotechnology, Inc., Santa Cruz CA) were purchased commercially. The immunohistochemical samples were counterstained with hematoxylin.

MMP inhibitor and MAPK inhibitor. MMP2 inhibitor, MMP9 inhibitor, and inhibitors GM6001, PD98059, SP600125, and SB203580 were purchased from Merck KGaA (Darmstadt, Germany). Concentrations were as follows: dimethyl sulfoxide, ×500; MMP2 inhibitor, 20 μM; MMP9 inhibitor, 2 μM; GM6001, 5 μM; PD98059, 20 μM; SP600125, 20 μM; and SB203580, 5 μM. Inhibitors were introduced into the medium mixture for the organotypic raft culture from day 1 to day 10.

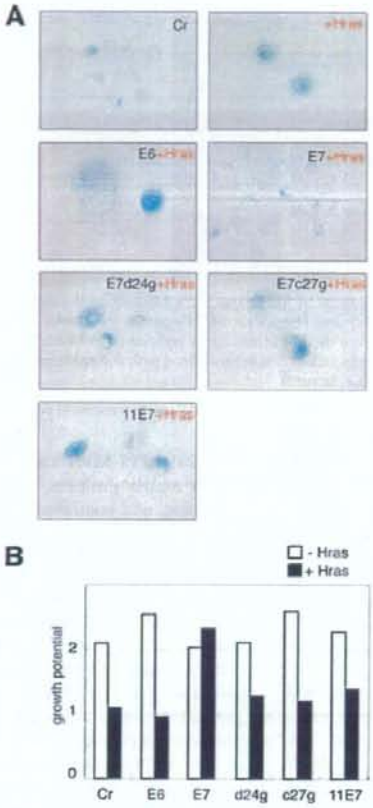

FIG. 1. Coexpression of HPV oncoproteins and H-rasV12 in primary HFKs. (A) Morphology and senescence induction of the HFKs expressing HPV oncoproteins and H-ras. The senescent cells were detected by SA-β-gal assay. The control cells (Cr) used in this and the following experiments were infected with two empty retroviral vectors, pLXSN and pLPCX. Magnification, ×200. (B) The effects of H-ras activation on the proliferation of the HFKs expressing HPV oncoproteins. At days 1 and 3 after they were seeded, the cells in the dishes were counted, and relative cell numbers (those at 1 day after seeding are set at 1) are indicated as a bar.

RESULTS

E7-expressing keratinocytes escaped from Ras-induced senescence through pRb degradation. We analyzed the effects of Ras activation on HPV-induced tumorigenesis. First, we introduced the active form of H-ras, which has one amino acid substitution (H-rasV12, consisting of a G-to-V change at position 12), into primary HFKs and analyzed the growth potential (Fig. 1). It was reported that the Ras activation in human primary cells induced premature senescence (49). In agreement with that report, the Ras activation could induce senescence-like growth arrest in HFKs. The Ras activation attenuated the cell growth and changed the cell to a flattened and enlarged senescence-like shape. The senescence induction could also be confirmed by SA-β-gal assay (Fig. 1A). Next, the H-rasV12 was introduced into the HFKs expressing HPV oncoprotein. Although Ras activation could induce senescence-like growth arrest in the HFKs expressing HPV18 E6 (18E6), 18E7 expression rescued the cells from senescence.

High-risk type E7 binds to and inactivates pRb and induces its degradation through the proteasome pathway (18). To investigate whether pRb inactivation was required for escape from Ras-induced senescence, we analyzed the effects of two 18E7 mutants (D24G and C27G) and low-risk HPV11 E7 (11E7) expression on Ras-induced senescence (Fig. 1). These E7 mutants could not inactivate the pRb (22, 31), and neither of them could eliminate the Ras-induced senescence, indicating that pRb inactivation was important for escape from senescence.

E7 has been reported to bind to other pocket protein family members (37). Although the degradation of pRb is specific to high-risk E7, we reported that p130 was targeted for degradation by both types of E7 (HPV18 E7 and HPV11 E7) in HFKs (52). In the same report, we demonstrated that the expression level of p107 was not modified by E7s. Considering these observations, the results shown above indicate that p107 and p130 were not involved in the Ras-induced senescence. This notion was supported by the observation that a pRb knockdown with a specific shRNA could eliminate the Ras-induced senescence (data not shown).

Coexpression of 18E7 and H-rasV12 conferred invasive potential on epidermis raft culture. We analyzed the effect of Ras activation on epidermis formation, using an organotypic raft culture system (Fig. 2A). With control HFKs, normal epidermal structure could be reproduced. The cells expressing H-rasV12 or both H-rasV12 and 18E6 could not be used for the construction of the raft culture because their growth potentials were severely retarded, as shown in Fig. 1B. The 18E7 expression induced hyperplasia in the epidermal layer as previously reported (52). The cells expressing both H-rasV12 and 18E7 showed hyperplasia and invaded the dermal layer that consisted of type I collagen and HFFs, suggesting that Ras activation conferred invasive potential on the cells expressing high-risk E7. Invasion induced by H-rasV12 and 18E7 was confirmed by an invasion assay using a Transwell coated with extracellular matrix (Matrigel; BD Biosciences, Franklin Lakes, NJ).

In contrast to the invasive potential observed for the HFKs, HeLa cells derived from HPV18-positive cervical carcinoma showed very weak invasion activity, even with the ectopic expression of H-rasV12 (Fig. 2B), which raised the possibility that the HFKs expressed E7 protein more abundantly than the HeLa cells. As shown in Fig. 2B, the expressions level of 18E7 in the HFKs was apparently lower than that in HeLa cells, suggesting that the 18E7 expression level in the HFKs was within the physiological level.

Ras activation was reported to contribute to the invasive potential of cancer cells by inducing MMPs through MAPK pathway activation (10). To investigate whether MMPs were induced in the epidermal layer of the raft culture expressing both H-rasV12 and 18E7, we performed immunohistochemical analyses for MMP2 and MMP9, which are type IV collagenases and major MMPs inducible by Ras (Fig. 3). MMP2 was constitutively expressed by the HFFs embedded in the dermal equivalent and was broadly distributed in the dermal layer. The expression of MMP9 was induced in the whole epidermal layer

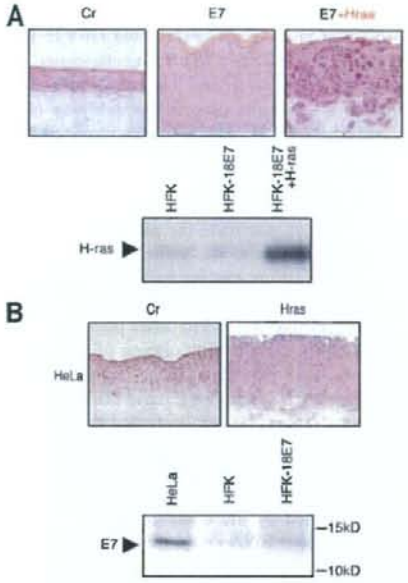

FIG. 2. Effects of Ras activation in E7-expressing cells were evaluated using raft culture. (A) HFKs expressing 18E7 and/or H-rasV12 were used for the raft culture construction. The cryosection (7 μm) was fixed with formaldehyde and stained with H&E. Magnifications in this and subsequent figures, ×100. H-ras expression in the cells was monitored by immunoblot analysis. (B) HeLa cells were used for the raft culture system. H-rasV12 was transduced by the retroviral vector pLPCX. 18E7 expression level was analyzed with an 18E7-specific polyclonal antibody. Cr, control.

by 18E7 expression. These MMPs might contribute to the invasive potential of the HFKs expressing both H-rasV12 and 18E7.

In the acquisition of invasive potential, the activation of MMPs through cleavage by other proteases is also involved (13). MT1-MMP is a matrix-anchored type of MMP, which is

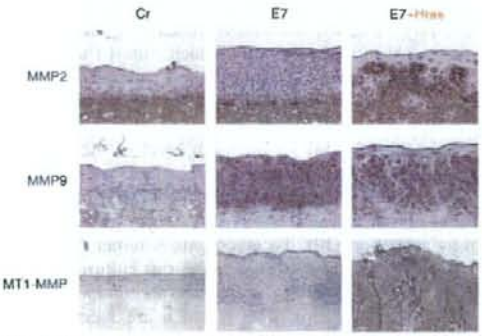

FIG. 3. Immunohistochemical analysis of MMP expression in the raft culture. MMP expression was detected by a TSA biotin system and is shown as a dark, brownish signal. The samples were counterstained with hematoxylin. Cr, control.

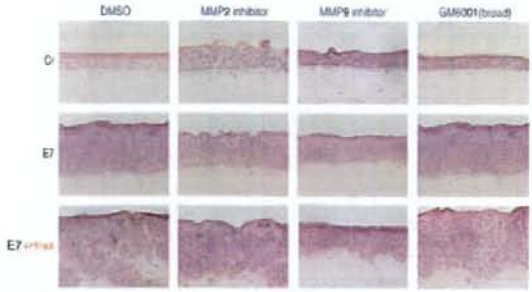

FIG. 4. Effects of MMP-specific inhibitors on the invasion induced by both 18E7 and H-rasV12. MMP-specific inhibitors were added to the raft culture medium from day 1 (described in Materials and Methods). The cryosection (7 μm) was fixed with formaldehyde and stained with H&E. Cr, control.

a major activator for MMP2 (26). MT1-MMP can also cleave other MMPs and extracellular matrix proteins, for example, fibronectin, laminin, and collagen, and contributes to cell invasiveness. We analyzed the MT1-MMP expression in the raft culture expressing H-rasV12 and 18E7 (Fig. 3). The expression of MT1-MMP was induced by H-rasV12 in the epidermal keratinocytes, especially at the boundary between the epidermal and the dermal layers. In the same sample, MMP2 also accumulated at the boundary (Fig. 3, E7+Hras panels), suggesting that the MT1-MMP induced by the Ras activation recruited the MMP2 expressed by the HFFs for its activation.

MMP upregulation confers invasive potential on the H-rasV12 and 18E7-coexpressing epidermis. To investigate whether the MMP induction described above was involved in the invasion potential, we analyzed the effects of MMP inhibitors on invasion (Fig. 4). The MMP2-specific inhibitor partially inhibited invasion; the MMP9-specific inhibitor strongly inhibited invasion, suggesting that the MMP9 induced by 18E7 contributed to invasion. However, induction of MMP9 might not be sufficient for invasion because the expression of 18E7 only could not confer the invasion potential on the keratinocytes. GM6001, which is a broad inhibitor of MMPs, suppressed invasion of MMP9. These results suggested that these MMPs cooperated with each other to promote the invasiveness of the HFKs expressing both H-rasV12 and 18E7.

MMP9 and MT1-MMP were induced through the MEK/ERK pathway. It is known that Ras induces MMP expression through the activation of the MAPK pathway (30). To investigate the involvement of MAPK activation in invasion, the effects of the MAPK-specific inhibitors on invasion potential were examined (Fig. 5). A MEK-specific inhibitor, PD98059, clearly suppressed the invasion capacity of the cells expressing both E7 and H-ras. A p38-specific inhibitor, SB203580, had no effect on invasiveness. SP600125, a JNK-specific inhibitor, inhibited normal epidermis formation, suggesting that the JNK activity was essential for the development of stratified epidermis as previously reported (58). These results indicate that the invasion potential was induced through the activation of the MEK/ERK pathway.

Next, the effects of the MAPK inhibitors on the expressions of MMP9 and MT1-MMP were analyzed by immunohisto-

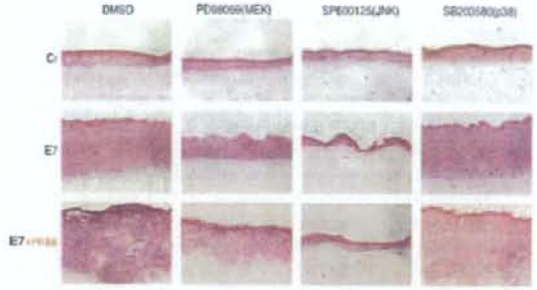

FIG. 5. Effects of MAPK-specific inhibitors on the invasion induced by both 18E7 and H-rasV12. MAPK-specific inhibitors were added to the raft culture medium from day 1. The cryosection (7 μm) was fixed with formaldehyde and stained with H&E. Cr. control.

chemical assay (Fig. 6). Expression of MMP9 (Fig. 6A) and MT1-MMP (Fig. 6B) was suppressed by PD98059, suggesting that their expression was induced through the activation of the MEK/ERK pathway.

18E7 and constitutive active MEK1-coexpressing epidermis partly reproduced the invasiveness of the H-rasV12 and HPV18 E7-coexpressing epidermis. The results shown above suggested that the invasiveness induced by H-rasV12 and 18E7 was mediated by the MMP activation through the MEK/ERK pathway. To examine whether the MEK/ERK activation could mimic the Ras activation for the induction of invasiveness, the

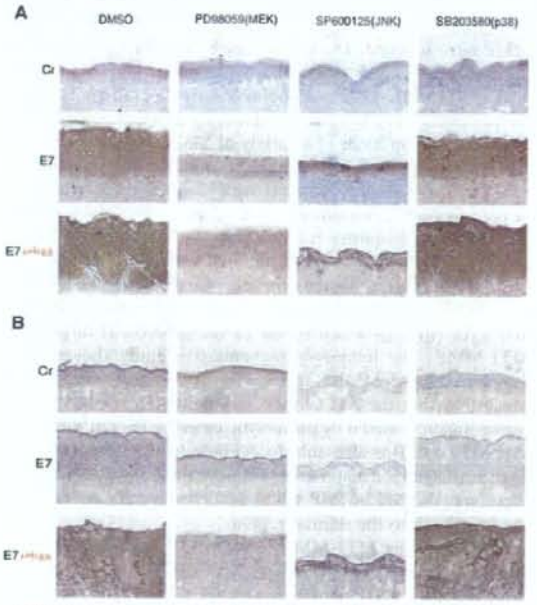

FIG. 6. Effects of the MAPK-specific inhibitors on the MMP expression. The MAPK-specific inhibitors were added to the raft culture medium from day 1. Immunohistochemical analyses were performed for MMP9 (A) and MT1-MMP (B). The samples were counterstained with hematoxylin. Cr. control.

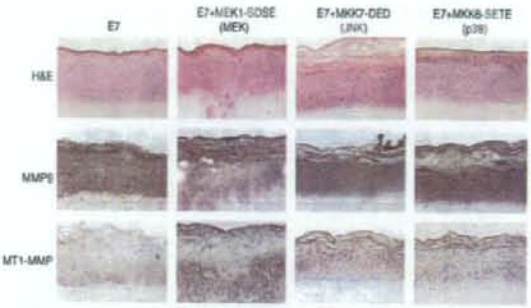

FIG. 7. Expressions of constitutive active MAPKs in the HPV18 E7-expressing keratinocytes. Invasion activity was monitored with the organotypic raft culture. The cryosection (7um) was fixed with formaldehyde and stained with H&E. MMP expression was monitored by immunohistochemical analysis, and the samples were counterstained with hematoxylin (MMP9 and MT1-MMP).

constitutively active mutant of MEK1, MKK7 or MKK6, was expressed in the HFKs expressing 18E7, and the raft culture was constructed with them (Fig. 7). The epidermis expressing MEK1-SDSE (the MEK1 constitutive active mutant) acquired invasive potential, and MT1-MMP expression was induced. MKK7-DED (for the JNK pathway) and MKK6-SETE (for the p38 pathway) expression did not induce the invasion. Although these results indicated the involvement of the MEK/ERK pathway in the induction of MT1-MMP and invasiveness, the invasion induced by the MEK1-SDSE was attenuated compared with that induced by H-rasV12 and 18E7 coexpression, suggesting that other pathways or factors in addition to MAPK activation contribute to the invasive potential in Ras activation. It was apparent that all of the MAPK mutants expressing epidermis showed a thickened cornified layer, suggesting that these MAPK pathways contribute to the differentiation program of epidermis in some part.

MMP9 induction was independent of pRb degradation. We investigated the mechanisms by which 18E7 induced MMP9 expression. A well-known activity of the high-risk E7 is its capacity to bind to and inactivate pRb. We therefore examined the effect of the pRb knockdown on the expression of MMP9. The raft culture with the pRb knockdown cells was established by using a retroviral vector expressing the shRNA targeted to pRb. The pRb expression level was monitored by immunoblot analysis with anti-pRb antibody (Fig. 8A). The pRb knockdown did not induce MMP9 in the epidermis, and the expression of low-risk HPV11 E7 that could not inactivate pRb induced MMP9 (Fig. 8B), suggesting that the upregulation of MMP9 by E7 was independent of the pRb degradation.

DISCUSSION

Cancer-prone status of HPV-infected cells. For HPV-induced carcinogenesis, the major viral oncoproteins E6 and E7 are pivotal; both E6 and E7 disturb the cell cycle checkpoint and the apoptosis induction, resulting in the augmentation of genetic instability. For the progression of carcinogenesis, it is believed that additional host mutations are required and that the ras family of proto-oncogenes is one of the major targets

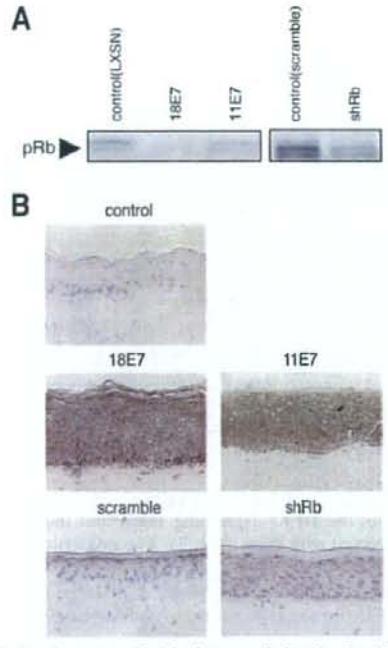

FIG. 8. Involvement of pRb downregulation in the E7-induced MMP9 expression. (A) The effect on pRb expression by E7 (derived from pLXSN) or shRNA targeted to pRb (shRb) (derived from pSIREN-RetroQ) was analyzed by immunoblotting. (B) HFKs expressing E7 or shRb were used to construct the raft culture. A random oligonucleotide was used as a control for the shRb (scramble).

for the mutations. Although Ras activation in HFKs induces premature senescence through the pRb-related pathway, the high-risk E7 oncoprotein could eliminate senescence induction and confer invasive potential on the HFKs in cooperation with Ras activation (Fig. 1 and 2). The results indicate that the HPV-infected cells that express E7 are tolerant of the Ras activation, which contributes to malignant conversion of the HPV-infected lesion. Other oncogenic stresses, such as the activations of Raf, ERK, or Akt, are also reported to induce "premature senescence" (5), and our observation suggested that the high-risk HPV-infected cells are tolerant of such stresses, which might confer the "cancer-prone" status on the HPV-infected cells.

It was reported that transformation by Ras activation in normal human cells requires p53 inactivation, pRb inactivation, c-*myc* activation, PP2A inactivation, and telomerase reactivation (20). Although our report indicated that the high-risk E7 expression, which induces pRb degradation and c-*myc* activation, conferred invasiveness on the HFKs in cooperation with the Ras activation, the combined expression of 18E7 and H-rasV12 is not sufficient for the induction of transformation. For the transformation, additional alterations of the host cells as well as high-risk E6 expression must be required. We are seeking such additional cellular factors that are involved in the multiple aspects of the malignant conversion, such as the cell motility, the metastasis conversion, and the evasion of the host immune system.

MMP induction and invasiveness. The acquisition of invasive potential by the coexpression of H-rasV12 and 18E7 resulted from MMP induction, which was supported by experiments with several MMP inhibitors (Fig. 4). MMP9 expression was upregulated by 18E7, but 18E7 expression by itself did not induce the invasiveness of the epidermal cells (Fig. 2, 3). Although this observation indicated that MMP9 expression was not sufficient for the acquisition of the invasive potential, its involvement in invasiveness was supported by the result of the MMP9-specific inhibitor (Fig. 4). It was reported that MMP9 was related not only to invasiveness but also to cell proliferation (8). The hyperplasia of epidermis induced by 18E7 expression was significantly suppressed by the MMP9-specific inhibitor (Fig. 4), suggesting that the MMP9 expression was also involved in the cell proliferation of epidermis. We reported that the 18E7-induced hyperplasia resulted from the degradation of pRb and p130 and that the low-risk HPV11 E7 caused mild hyperplasia by inactivating p130 (52). The induction of MMP9 was independent of pRb inactivation, and HPV11 E7 had a potential to induce MMP9 expression (Fig. 8), indicating a possibility that MMP9 induction was a common feature of both types of E7 and that induction is involved in E7-mediated hyperplasia.

E7-mediated MMP induction has been reported with other types of HPVs. HPV16 E7 induced MT1-MMP expression in keratinocytes; such an effect was not evident for HPV18-positive HeLa cells (50, 57). It was reported that the expression of HPV8 E7, which is a cutaneous-type HPV, was enough to confer the invasive potential on the epithelial cells in the organotypic raft culture (1), in which MMP1, MMP8, and MT1-MMP were induced. The differences between E7 functions in the invasiveness of various HPV types might be due to their host cell tropism, and it will be necessary to examine the key factor involved in the MMP induction by E7s. An examination of the expression levels of a variety of MMPs in the epidermal cells expressing both 18E7 and H-ras will also be required.

MT1-MMP was induced by H-rasV12 in the epidermal cells of the raft culture, especially at the basal layer cells in contact with the dermal equivalent (Fig. 3). It was reported that MT1-MMP was highly expressed at the cell surface of cancer cells (26). MMP2 was expressed from the fibroblasts embedded in the dermal equivalent and was broadly distributed in the dermal layer (Fig. 3), which is one of the proteolytic targets of MT1-MMP. The immunohistochemical staining showed the accumulation of MMP2 at the region of basal membrane, suggesting that the MT1-MMP recruited the MMP2 at the region and activated it by proteolytic cleavage (51). It is known that MT1-MMP is also able to degrade type I collagen (24). Type I collagen is a major component of the dermal region (6); therefore, the MT1-MMP might function as a "pioneer" for the invasion into the dermal region.

In contrast to MT1-MMP, both MMP2 and MMP9 are known as type IV collagenases (13, 53). Type IV collagen localizes at the basal membrane (6), and both MMPs might be involved in the degradation of basal membrane at the early stage of invasion. MMP2 was also known to activate MMP9 (16). A recent study reported that MMP2 could upregulate cell migration in vitro in cooperation with MMP9 (42). That re-

port, using the knockout mouse for MMP2 and MMP9, indicated their contribution to the invasiveness (33). These reports indicate that a cooperative function between MMP2 and MMP9 is important for invasiveness.

The MEK/ERK pathway was involved in the MMP induction by H-ras and 18E7. The expression of MMP9 and MT1-MMP was upregulated through the MEK/ERK pathway. The upstream events, however, might be distinct, because they were differentially regulated by 18E7 and H-ras (Fig. 3). The constitutive active mutant of MEK could induce significant but weak invasion in cooperation with 18E7 (Fig. 7), suggesting that the other pathways triggered by the Ras activation were involved in the strong invasiveness observed for the cells expressing both H-rasV12 and 18E7. The p38 pathway appeared not to be involved in the epidermal formation and the invasion potential (Fig. 5). JNK activation seemed to be essential for the proliferation of stratified epithelial cells, because SP600125, a JNK inhibitor, drastically suppressed epidermal formation, which is consistent with a report that the JNK activity was essential for the development of stratified epidermis (17, 58).

We reproduced a portion of multistep carcinogenesis, "the acquisition of invasiveness," by introducing 18E7 and H-rasV12 into the raft culture system. The raft culture is suitable to analyze the cell invasion and motility in a semiphysiological condition and useful for the screening of the drugs against invasiveness.

ACKNOWLEDGMENTS

This work is supported by Japanese Grants-in-Aid for Scientific Research from the Ministry of Education, Culture, Sports, Science, and Technology and by the Japanese Ministry of Health and Welfare. S.Y. and H.N. are supported by the 21st Century COE Program of JSPS.

Activated H-*ras* gene was provided by Ishikawa. Several DNAs of MAPK mutants were provided by Nishida.

REFERENCES

1. **Akgül, B., R. García-Escudero, L. Ghali, H. J. Pfister, P. G. Fuchs, H. Navsaria, and A. Storey.** 2005. The E7 protein of cutaneous human papillomavirus type 8 causes invasion of human keratinocytes into the dermis in organotypic cultures of skin. Cancer Res. **65:**2216–2223.
2. **Alonio, L. V., M. A. Dalbert, D. Mural, J. Bartt, O. Bazán, G. Dominguez, and A. R. Teyssié.** 2003. Ha-ras oncogene mutation associated to progression of papillomavirus induced lesions of uterine cervix. J. Clin. Virol. **27:**263–269.
3. **Bos, J. L.** 1989. ras oncogenes in human cancer: a review. Cancer Res. **49:**4682–4689.
4. **Cairns, J.** 1975. Mutation selection and the natural history of cancer. Nature **255:**197–200.
5. **Campisi, J., and F. d'Adda di Fagagna.** 2007. Cellular senescence: when bad things happen to good cells. Nat. Rev. Mol. Cell Biol. **8:**729–740.
6. **Canty, E. G., and K. E. Kadler.** 2005. Procollagen trafficking, processing and fibrillogenesis. J. Cell Sci. **118:**1341–1353.
7. **Cole, S. T., and O. Danos.** 1987. Nucleotide sequence and comparative analysis of the human papillomavirus type 18 genome. Phylogeny of papillomaviruses and repeated structure of the E6 and E7 gene products. J. Mol. Biol. **193:**599–608.
8. **Coussens, L. M., C. L. Tinkle, D. Hanahan, and Z. Werb.** 2000. MMP-9 supplied by bone marrow-derived cells contributes to skin carcinogenesis. Cell **103:**481–490.
9. **Dollard, S. C., J. L. Wilson, L. M. Demeter, W. Bonnez, R. C. Reichman, T. R. Broker, and L. T. Chow.** 1992. Production of human papillomavirus and modulation of the infectious program in epithelial raft cultures. Genes Dev. **6:**1131–1142.
10. **Downward, J.** 2003. Targeting RAS signalling pathways in cancer therapy. Nat. Rev. Cancer **3:**11–22.
11. **Duensing, S., A. Duensing, E. R. Flores, A. Do, P. F. Lambert, and K. Münger.** 2001. Centrosome abnormalities and genomic instability by episomal expression of human papillomavirus type 16 in raft cultures of human keratinocytes. J. Virol. **75:**7712–7716.
12. **Dyson, N., P. M. Howley, K. Münger, and E. Harlow.** 1989. The human papilloma virus-16 E7 oncoprotein is able to bind to the retinoblastoma gene product. Science **243:**934–937.
13. **Egeblad, M., and Z. Werb.** 2002. New functions for the matrix metalloproteinases in cancer progression. Nat. Rev. Cancer **2:**161–174.
14. **Fehrmann, F., and L. A. Laimins.** 2003. Human papillomaviruses: targeting differentiating epithelial cells for malignant transformation. Oncogene **22:**5201–5207.
15. **Flores, E. R., and P. F. Lambert.** 1997. Evidence for a switch in the mode of human papillomavirus type 16 DNA replication during the viral life cycle. J. Virol. **71:**7167–7179.
16. **Fridman, R., M. Toth, D. Pena, and S. Mobashery.** 1995. Activation of progelatinase B (MMP-9) by gelatinase A (MMP-2). Cancer Res. **55:**2548–2555.
17. **Gazel, A., T. Banno, R. Walsh, and M. Blumenberg.** 2006. Inhibition of JNK promotes differentiation of epidermal keratinocytes. J. Biol. Chem. **281:**20530–20541.
18. **Gonzalez, S. L., M. Stremlau, X. He, J. R. Basile, and K. Münger.** 2001. Degradation of the retinoblastoma tumor suppressor by the human papillomavirus type 16 E7 oncoprotein is important for functional inactivation and is separable from proteasomal degradation of E7. J. Virol. **75:**7583–7591.
19. **Greenhalgh, D. A., X. J. Wang, J. A. Rothnagel, J. N. Eckhardt, M. I. Quintanilla, J. L. Barber, D. S. Bundman, M. A. Longley, R. Schlegel, and D. R. Roop.** 1994. Transgenic mice expressing targeted HPV-18 E6 and E7 oncogenes in the epidermis develop verrucous lesions and spontaneous, Ha-ras-activated papillomas. Cell Growth Differ. **5:**667–675.
20. **Hahn, W. C., C. M. Counter, A. S. Lundberg, R. L. Beijersbergen, M. W. Brooks, and R. A. Weinberg.** 1999. Creation of human tumour cells with defined genetic elements. Nature **400:**464–468.
21. **Harada, T., O. Matsuzaki, H. Hayashi, S. Sugano, A. Matsuda, and E. Nishida.** 2003. AKRL1 and AKRL2 activate the JNK pathway. Genes Cells **8:**493–500.
22. **Heck, D. V., C. L. Yee, P. M. Howley, and K. Münger.** 1992. Efficiency of binding the retinoblastoma protein correlates with the transforming capacity of the E7 oncoproteins of the human papillomaviruses. Proc. Natl. Acad. Sci. USA **89:**4442–4446.
23. **Helt, A. M., J. O. Funk, and D. A. Galloway.** 2002. Inactivation of both the retinoblastoma tumor suppressor and p21 by the human papillomavirus type 16 E7 oncoprotein is necessary to inhibit cell cycle arrest in human epithelial cells. J. Virol. **76:**10559–10568.
24. **Hotary, K., E. Allen, A. Punturieri, I. Yana, and S. J. Weiss.** 2000. Regulation of cell invasion and morphogenesis in a three-dimensional type I collagen matrix by membrane-type matrix metalloproteinases 1, 2, and 3. J. Cell Biol. **149:**1309–1323.
25. **Howley, P. M., and D. Lowy.** 2001 Papillomaviruses and their replication, p. 2197–2229. *In* D. M. Knipe and P. M. Howley (ed.), Fields virology, 4th ed. Lippincott Williams & Wilkins, Baltimore, MD.
26. **Itoh, Y., and M. Seiki.** 2006. MT1-MMP: a potent modifier of pericellular microenvironment. J. Cell Physiol. **206:**1–8.
27. **Jones, D. L., R. M. Alani, and K. Münger.** 1997. The human papillomavirus E7 oncoprotein can uncouple cellular differentiation and proliferation in human keratinocytes by abrogating p21Cip1-mediated inhibition of cdk2. Genes Dev. **11:**2101–2111.
28. **Kiyono, T., A. Hiraiwa, M. Fujita, Y. Hayashi, T. Akiyama, and M. Ishibashi.** 1997. Binding of high-risk human papillomavirus E6 oncoproteins to the human homologue of the Drosophila discs large tumor suppressor protein. Proc. Natl. Acad. Sci. USA **94:**11612–11616.
29. **Klingelhutz, A. J., S. A. Foster, and J. K. McDougall.** 1996. Telomerase activation by the E6 gene product of human papillomavirus type 16. Nature **380:**79–82.
30. **Kranenburg, O., M. F. Gebbink, and E. E. Voest.** 2004. Stimulation of angiogenesis by Ras proteins. Biochim. Biophys. Acta **1654:**23–37.
31. **Lee, J. O., A. A. Russo, and N. P. Pavletich.** 1998. Structure of the retinoblastoma tumour-suppressor pocket domain bound to a peptide from HPV E7. Nature **391:**859–865.
32. **Lee, S. S., R. S. Weiss, and R. T. Javier.** 1997. Binding of human virus oncoproteins to hDlg/SAP97, a mammalian homolog of the Drosophila discs large tumor suppressor protein. Proc. Natl. Acad. Sci. USA **94:**6670–6675.
33. **Masson, V., L. R. de la Ballina, C. Munaut, B. Wielockx, M. Jost, C. Maillard, S. Blacher, K. Bajou, T. Itoh, S. Itohara, Z. Werb, C. Libert, J. M. Foidart, and A. Noël.** 2005. Contribution of host MMP-2 and MMP-9 to promote tumor vascularization and invasion of malignant keratinocytes. FASEB J. **19:**234–236.
34. **Medina-Martinez, O., V. Vallejo, M. C. Guido, and A. García-Carrancá.** 1997. Ha-ras oncogene-induced transcription of human papillomavirus type 18 E6 and E7 oncogenes. Mol. Carcinog. **19:**83–90.
35. **Meyers, C., M. G. Frattini, J. B. Hudson, and L. A. Laimins.** 1992. Biosynthesis of human papillomavirus from a continuous cell line upon epithelial differentiation. Science **257:**971–973.
36. **Münger, K., A. Baldwin, K. M. Edwards, H. Hayakawa, C. L. Nguyen, M. Owens, M. Grace, and K. Huh.** 2004. Mechanisms of human papillomavirus-induced oncogenesis. J. Virol. **78:**11451–11460.

37. **Münger, K., J. R. Basile, S. Duensing, A. Eichten, S. L. Gonzalez, M. Grace, and L. V. Zancy.** 2001. Biological activities and molecular targets of the human papillomavirus E7 oncoprotein. Oncogene **20:**7888–7898.
38. **Nguyen, M. L., M. M. Nguyen, D. Lee, A. E. Griep, and P. F. Lambert.** 2003. The PDZ ligand domain of the human papillomavirus type 16 E6 protein is required for E6's induction of epithelial hyperplasia in vivo. J. Virol. **77:**6957–6964.
39. **O'Connor, M. J., W. Stünkel, C. H. Koh, H. Zimmermann, and H. U. Bernard.** 2000. The differentiation-specific factor CDP/Cut represses transcription and replication of human papillomaviruses through a conserved silencing element. J. Virol. **74:**401–410.
40. **Pietenpol, J. A., R. W. Stein, E. Moran, P. Yaciuk, R. Schlegel, R. M. Lyons, M. R. Pittelkow, K. Münger, P. M. Howley, and H. L. Moses.** 1990. TGF-beta 1 inhibition of c-myc transcription and growth in keratinocytes is abrogated by viral transforming proteins with pRB binding domains. Cell **61:**777–785.
41. **Pim, D., and L. Banks.** 1991. Loss of HPV-16 E7 dependence in cells transformed by HPV-16 E7 plus EJ-ras correlates with increased c-myc expression. Oncogene **6:**589–594.
42. **Robinson, C. M., A. M. Stone, J. D. Shields, S. Huntley, I. C. Paterson, and S. S. Prime.** 2003. Functional significance of MMP-2 and MMP-9 expression by human malignant oral keratinocyte cell lines. Arch. Oral Biol. **48:**779–786.
43. **Ruesch, M. N., F. Stubenrauch, and L. A. Laimins.** 1998. Activation of papillomavirus late gene transcription and genome amplification upon differentiation in semisolid medium is coincident with expression of involucrin and transglutaminase but not keratin-10. J. Virol. **72:**5016–5024.
44. **Sagae, S., R. Kudo, N. Kuzumaki, T. Hisada, Y. Mugikura, T. Nihei, T. Takeda, and M. Hashimoto.** 1990. Ras oncogene expression and progression in intraepithelial neoplasia of the uterine cervix. Cancer **66:**295–301.
45. **Scheffner, M., B. A. Werness, J. M. Huibregtse, A. J. Levine, and P. M. Howley.** 1990. The E6 oncoprotein encoded by human papillomavirus types 16 and 18 promotes the degradation of p53. Cell **63:**1129–1136.
46. **Schiffman, M., P. E. Castle, J. Jeronimo, A. C. Rodriguez, and S. Wacholder.** 2007. Human papillomavirus and cervical cancer. Lancet **370:**890–907.
47. **Schreiber, K., R. E. Cannon, T. Karrison, G. Beck-Engeser, D. Huo, R. W. Tennant, H. Jensen, W. M. Kast, T. Krausz, S. C. Meredith, L. Chen, and H. Schreiber.** 2004. Strong synergy between mutant ras and HPV16 E6/E7 in the development of primary tumors. Oncogene **23:**3972–3979.
48. **Schubbert, S., K. Shannon, and G. Bollag.** 2007. Hyperactive Ras in developmental disorders and cancer. Nat. Rev. Cancer **7:**295–308.
49. **Serrano, M., A. W. Lin, M. E. McCurrach, D. Beach, and S. W. Lowe.** 1997. Oncogenic ras provokes premature cell senescence associated with accumulation of p53 and p16INK4a. Cell **88:**593–602.
50. **Smola-Hess, S., J. Pahne, C. Mauch, P. Zigrino, H. Smola, and H. J. Pfister.** 2005. Expression of membrane type 1 matrix metalloproteinase in papillomavirus-positive cells: role of the human papillomavirus (HPV) 16 and HPV8 E7 gene products. J. Gen. Virol. **86:**1291–1296.
51. **Taniwaki, K., H. Fukamachi, K. Komori, Y. Ohtake, T. Nonaka, T. Sakamoto, T. Shiomi, Y. Okada, T. Itoh, S. Itohara, M. Seiki, and I. Yana.** 2007. Stroma-derived matrix metalloproteinase (MMP)-2 promotes membrane type 1-MMP-dependent tumor growth in mice. Cancer Res. **67:**4311–4319.
52. **Ueno, T., K. Sasaki, S. Yoshida, N. Kajitani, A. Satsuka, H. Nakamura, and H. Sakai.** 2006. Molecular mechanisms of hyperplasia induction by human papillomavirus E7. Oncogene **25:**4155–4164.
53. **Werb, Z.** 1997. ECM and cell surface proteolysis: regulating cellular ecology. Cell **91:**439–442.
54. **Woodman, C. B., S. I. Collins, and L. S. Young.** 2007. The natural history of cervical HPV infection: unresolved issues. Nat. Rev. Cancer **7:**11–22.
55. **Yokota, J., and T. Sugimura.** 1993. Multiple steps in carcinogenesis involving alterations of multiple tumor suppressor genes. FASEB J. **7:**920–925.
56. **Yukawa, K., K. Butz, T. Yasui, H. Kikutani, and F. Hoppe-Seyler.** 1996. Regulation of human papillomavirus transcription by the differentiation-dependent epithelial factor Epoc-1/skn-1a. J. Virol. **70:**10–16.
57. **Zhai, Y., K. B. Hotary, B. Nan, F. X. Bosch, N. Muñoz, S. J. Weiss, and K. R. Cho.** 2005. Expression of membrane type 1 matrix metalloproteinase is associated with cervical carcinoma progression and invasion. Cancer Res. **65:**6543–6550.
58. **Zhang, J. Y., C. L. Green, S. Tao, and P. A. Khavari.** 2004. NF-κB RelA opposes epidermal proliferation driven by TNFR1 and JNK. Genes Dev. **1:**17–22.
59. **zur Hausen, H.** 1996. Papillomavirus infections: a major cause of human cancers. Biochim. Biophys. Acta **1288:**F55–F78.

JOURNAL OF VIROLOGY, Sept. 2008, p. 8349–8361 Vol. 82, No. 17
0022-538X/08/$08.00+0 doi:10.1128/JVI.00306-08

Intramembrane Processing by Signal Peptide Peptidase Regulates the Membrane Localization of Hepatitis C Virus Core Protein and Viral Propagation▽

Kiyoko Okamoto,[1]† Yoshio Mori,[1]† Yasumasa Komoda,[1] Toru Okamoto,[1] Masayasu Okochi,[2] Masatoshi Takeda,[2] Tetsuro Suzuki,[3] Kohji Moriishi,[1] and Yoshiharu Matsuura[1]*

Department of Molecular Virology, Research Institute for Microbial Diseases,[1] and Department of Post-Genomics and Diseases, Division of Psychiatry and Behavioral Proteomics, Graduate School of Medicine,[2] Osaka University, Osaka, and Department of Virology II, National Institute of Infectious Diseases, Tokyo,[3] Japan

Received 12 February 2008/Accepted 11 June 2008

Hepatitis C virus (HCV) core protein has shown to be localized in the detergent-resistant membrane (DRM), which is distinct from the classical raft fraction including caveolin, although the biological significance of the DRM localization of the core protein has not been determined. The HCV core protein is cleaved off from a precursor polyprotein at the lumen side of Ala[191] by signal peptidase and is then further processed by signal peptide peptidase (SPP) within the transmembrane region. In this study, we examined the role of SPP in the localization of the HCV core protein in the DRM and in viral propagation. The C terminus of the HCV core protein cleaved by SPP in 293T cells was identified as Phe[177] by mass spectrometry. Mutations introduced into two residues (Ile[176] and Phe[177]) upstream of the cleavage site of the core protein abrogated processing by SPP and localization in the DRM fraction. Expression of a dominant-negative SPP or treatment with an SPP inhibitor, L685,458, resulted in reductions in the levels of processed core protein localized in the DRM fraction. The production of HCV RNA in cells persistently infected with strain JFH-1 was impaired by treatment with the SPP inhibitor. Furthermore, mutant JFH-1 viruses bearing SPP-resistant mutations in the core protein failed to propagate in a permissive cell line. These results suggest that intramembrane processing of HCV core protein by SPP is required for the localization of the HCV core protein in the DRM and for viral propagation.

The hepatitis C virus (HCV), which has infected an estimated 170 million people worldwide, leads to chronic hepatitis, which in turn causes severe liver diseases, including steatosis, cirrhosis, and eventually hepatocellular carcinoma (47). HCV possesses a positive-sense single-stranded RNA with a nucleotide length of 9.6 kb, which encodes a single large precursor polyprotein composed of about 3,000 amino acids. The viral polyprotein is processed by cellular and viral proteases into structural and nonstructural proteins (24). The development of efficient therapies for hepatitis C had been hampered by the lack of a reliable cell culture system, as well as by the absence of a small-animal model. Lohmann et al. established an HCV replicon, which consisted of an antibiotic selection marker and a genotype 1b HCV RNA, and showed that it replicated autonomously in the intracellular compartments of a human hepatoma cell line, Huh7 (16). The replicon system has been used as an important tool in the investigation of HCV replication, and it has served as a cell-based assay system for the evaluation of antiviral compounds. Recently, cell culture systems for in vitro replication and infectious-virus production were established based on the full-length HCV genome of a genotype 2a isolate, which was recovered from a fulminant hepatitis C patient (15, 45, 50). However, the molecular mechanism of the HCV life cycle in host cells has not been well characterized.

Several viruses have been reported to utilize a lipid raft composed of cholesterol and sphingolipids upon entry (34). The lipid raft is characterized by resistance to nonionic detergents at 4°C and includes caveolin, glycolipids, and other substances (40). Several nonenveloped viruses enter cells through a caveola/raft-mediated endosome, designated the caveosome, and then translocate to the endoplasmic reticulum (ER), endosome, or nucleus (34, 35), although enveloped viruses generally enter host cells through a clathrin-dependent pathway (18). HCV is enclosed by a host cell-derived membrane and belongs to the family *Flaviviridae*. Several reports suggest that HCV enters host cells through general endocytosis, such as by a clathrin-mediated pathway (5, 6, 22). However, HCV has been suggested to replicate on a detergent-resistant membrane (DRM), including some characteristic membrane structures such as lipid rafts and membranous webs (8, 9, 38). In a previous report, an HCV replication complex prepared from a cell fraction treated with a nonionic detergent was shown to be enzymatically active (2). HCV nonstructural proteins remodel the intracellular membrane to form a replication complex that includes several host proteins (8, 46). The HCV core protein has a C-terminal transmembrane region that is anchored on intracellular compartments such as the ER and mitochondria and on the surfaces of lipid droplets (10, 30, 42). Recent studies have indicated that assembly of HCV particles occurs around lipid droplets that are surrounded by the remodeled membranes (23). Although the HCV core protein functions as a capsid protein, it is found in the DRM fraction, which is

* Corresponding author. Mailing address: Department of Molecular Virology, Research Institute for Microbial Diseases, Osaka University, 3-1 Yamada-oka, Suita, Osaka 565-0871, Japan. Phone: 81-6-6879-8340. Fax: 81-6-6879-8269. E-mail: matsuura@biken.osaka-u.ac.jp.
† K. Okamoto and Y. Mori contributed equally to this work.
▽ Published ahead of print on 18 June 2008.